

Evaluating Small Vision-Language Models on Distance-Dependent Traffic Perception

NIKOS THEODORIDIS^{1,2,3} (Graduate Student Member, IEEE), TIM BROPHY^{1,2,3} (Member, IEEE), REENU MOHANDAS^{1,2,3} (Member, IEEE), GANESH SISTU^{1,2,4}, FIACHRA COLLINS⁴, ANTHONY SCANLAN^{1,2}, CIARÁN EISING^{1,2,3} (Senior Member, IEEE)

¹Department of Electronic and Computer Engineering, University of Limerick, Castletroy, Co. Limerick V94 T9PX, Ireland

²Data Driven Computer Engineering Research Centre, University of Limerick, Castletroy, Co. Limerick V94 T9PX, Ireland

³Lero, The Irish Software Research Centre, University of Limerick, Limerick V94 NYD3, Ireland

⁴Valeo Vision Systems, Dunmore Road, Tuam, Co. Galway H54 Y276, Ireland

CORRESPONDING AUTHOR: NIKOS THEODORIDIS (e-mail: theodoridis.nikolaos@ul.ie).

This work was supported in part by Science Foundation Ireland under Grant 13/RC/2094_P2 and co-funded under the European Regional Development Fund through the Southern and Eastern Regional Operational Programme to Lero - the Science Foundation Ireland Research Centre for Software, and in part by Valeo Vision Systems.

ABSTRACT Vision-Language Models (VLMs) are becoming increasingly powerful, demonstrating strong performance on a variety of tasks that require both visual and textual understanding. Their strong generalisation abilities make them a promising component for automated driving systems, which must handle unexpected corner cases. However, to be trusted in such safety-critical applications, a model must first possess a reliable perception system. Moreover, since critical objects and agents in traffic scenes are often at a distance, we require systems that are not “shortsighted”, i.e., systems with strong perception capabilities at both close (up to 20 meters) and long (30+ meters) range. With this in mind, we introduce **Distance-Annotated Traffic Perception Question Answering (DTPQA)**, the first Visual Question Answering (VQA) benchmark focused solely on perception-based questions in traffic scenes, enriched with distance annotations. By excluding questions that require reasoning, we ensure that model performance reflects perception capabilities alone. Since automated driving hardware has limited processing power and cannot support large VLMs, our study centers on smaller VLMs. More specifically, we evaluate several state-of-the-art (SOTA) small VLMs on DTPQA and show that, despite the simplicity of the questions, these models significantly underperform compared to humans (~60% average accuracy for the best-performing small VLM versus ~85% human performance). However, it is important to note that the human sample size was relatively small, which imposes statistical limitations. We also identify specific perception tasks, such as distinguishing left from right, that remain particularly challenging for these models. We hope our findings will encourage further research into improving the perception capabilities of small VLMs in traffic scenarios, ultimately making them more suitable for automated driving applications.

INDEX TERMS Automated Driving, Perception, Vision-Language Models, VQA Benchmark

I. INTRODUCTION

Vision-Language Models have recently made remarkable progress across a wide range of tasks, from general Visual Question Answering (VQA) to complex analysis and reasoning over scientific charts [1–6]. This strong performance is partly due to the pretrained Large Language Models (LLMs) that Vision-Language Models (VLMs) use as backbones, inheriting their powerful reasoning and gener-

alisation abilities. The most common benchmarks used to evaluate VLMs typically require a combination of strong perception and reasoning capabilities, as well as advanced world knowledge [7–14]; however, this combination makes it difficult to pinpoint exactly where a model excels or falls short.

Some recent studies focus exclusively on the perception capabilities of VLMs and show that these remain limited,

particularly when it comes to fine-grained image details [15–19]. The perception abilities of small VLMs (fewer than 4 billion parameters) are even less explored, as most existing research focuses on large state-of-the-art (SOTA) models. This lack of attention hinders the adoption of VLMs, especially smaller ones, in safety-critical applications that demand a robust and trustworthy perception system.

Automated driving is one such application where VLMs could serve as a valuable component of the self-driving stack. The self-driving stack consists of the following layers [20]:

- **Sensing**, which includes the sensors mounted on the car (cameras, LiDARs, radars, etc.).
- **Perception**, comprising algorithms (e.g., object detection, segmentation) that receive the sensory input and create a 3D map.
- **Localisation**, comprising algorithms that, based on the perception input, calculate the exact position and orientation of the ego-vehicle.
- **Planning**, comprising algorithms that, based on the perception input and knowledge of the ego-vehicle’s position, plan its future trajectory.
- **Control**, which includes components that translate the defined plan into low-level actions (steering, accelerating, braking).

The strong reasoning and generalisation abilities of VLMs make them a promising component for the planning layer in the self-driving stack [21, 22]. Specifically, a VLM could be utilised as a high-level planner, where it first interprets the raw sensor input (i.e., perception) and then plans the desired action in natural language. This high-level decision could then be used, along with the raw sensory input, by other low-level components of the planning layer to predict the desired waypoints for the future trajectory. The work of Jiang *et al.* investigates this exact use case [21].

However, the limited perceptual capabilities of current VLMs make them unreliable for deployment in high-risk settings such as automated driving, even in expected scenarios. Even if a VLM possesses strong reasoning abilities, it must first correctly perceive its environment before it can make appropriate driving decisions. For instance, consider a scenario that falls under the known-unsafe category of Safety Of The Intended Functionality (SOTIF): a pedestrian crossing the road (an expected scenario) at a long range (30–50 meters), where the model fails to detect them. In such a case, no matter how strong its reasoning capabilities are, they would be of little use in enabling the system to decide that it should brake.

Moreover, the hardware typically used in self-driving vehicles imposes strict constraints on the size of models that can be deployed on it. For instance, a commonly used hardware platform for self-driving cars is the NVIDIA Jetson Orin [23]. Even the most powerful variant, the Jetson AGX Orin, provides only 64 GB of unified memory shared between its CPU and GPU. SOTA large VLMs require significantly

more memory. For example, InternVL3-78B [5] would need approximately 156 GB of VRAM just to load its parameters in bfloat16 precision (2 bytes per parameter for 78 billion parameters), which far exceeds the memory capacity of the Jetson AGX Orin. When additional memory requirements, such as for activations storage and other components of the self-driving stack, are considered to be running concurrently, it becomes clear that deploying such large models is infeasible.

Due to these limitations, our study focuses exclusively on small VLMs that can perform inference reliably on hardware like the Jetson AGX Orin and even on less powerful variants. More specifically, we study the perception-only capabilities of small, SOTA VLMs in traffic scenes. We assert that before trusting a VLM to participate in crucial driving decisions, we should be confident that it has a strong perception system and can comprehend the complex visual input of a traffic scene. This also requires the model not to be “shortsighted,” as traffic scenes often include crucial objects and agents that are at a distance. We, therefore, ask the following question: **Can small VLMs answer very simple (yet crucial) questions about traffic scenes that require only a good perception system, and how does their performance degrade as the distance of the object in question increases?** To investigate this, we need a VQA benchmark that meets three specific criteria: (a) it must include trivial, perception-only visual questions that do not require reasoning; (b) all samples should relate to traffic scenes, with questions crucial for driving decisions (e.g., not questions like “What colour is the car?”); and (c) it must contain distance annotations for each sample.

Since no existing VQA benchmark satisfies all these requirements, we introduce a new benchmark: Distance-Annotated Traffic Perception Question Answering (DTPQA). Specifically, DTPQA consists of trivial visual questions, most of which can be answered by any human at a glance, or after a closer look when there are distant objects, but are nonetheless crucial for driving decisions. Each DTPQA sample consists of (a) an image, (b) a question, (c) the ground truth answer, and (d) the distance of the object in question, enabling analysis of how VLM performance degrades with increasing object distance.

Additionally, for these models to be trusted in safety-critical applications, their perception capabilities should not be sensitive to how a question is phrased. To this end, we investigate if small, semantically equivalent modifications to DTPQA questions affect model performance on simple visual tasks, in order to assess their robustness.

To summarise, our contributions are as follows:

- 1) We introduce a novel benchmark, DTPQA, which, to the best of our knowledge, is the first VQA benchmark containing perception-only, trivial but crucial questions for traffic scenes with distance annotations.
- 2) We evaluate state-of-the-art small VLMs on our benchmark and draw insightful conclusions from the results.

- 3) We measure human performance on our benchmark to establish its ceiling performance.
- 4) We examine if small, semantically preserving modifications to questions affect model performance on DTPQA.

II. RELATED WORK

VLMs have made remarkable progress in recent years by leveraging the power of strong LLMs as backbones. Most modern open-source VLMs follow a similar high-level architecture that combines a visual encoder (typically a CLIP-like model [24]) with an LLM, using a projector to map visual features into the input space of the LLM [25–29]. This approach has demonstrated impressive results across a variety of tasks, such as image captioning, visual question answering, visual reasoning, chart and diagram understanding, and document or Optical Character Recognition (OCR) based QA, that require integrating multiple skills. Simultaneously, the number of benchmarks for evaluating such models has grown significantly [7–14], most of which require a combination of perception, reasoning, and advanced world knowledge to be solved.

A. Perception Capabilities of VLMs

A few studies have specifically investigated the perception capabilities of VLMs. One line of research evaluates large SOTA VLMs on simple visual tasks. For example, Rahmazadehgervi *et al.* [15] evaluated several SOTA VLMs on trivial visual questions, such as identifying the circled letter in a word or counting overlapping circles, that are easy for humans to answer at a glance. Their results showed that models like GPT-4o [1] and Claude-3.5-Sonnet [30] struggle significantly with such tasks. Kamoi *et al.* [18] introduced VisOnlyQA, a benchmark developed to assess the standalone visual perception abilities of VLMs. They evaluated GPT-4o [1], Gemini 1.5 Pro [31], and InternVL2-76B [32], concluding that all of them exhibited weak perception capabilities. Moreover, they found that fine-tuning on perception-only benchmarks did not sufficiently address the problem. However, these studies focus exclusively on large VLMs and not on traffic scenes, leaving a gap that our work aims to fill. In addition, none of these studies investigates how perception degrades with distance, which is one of the main focuses of our study.

Another line of research interprets the perception mechanisms of these models and explores ways to improve them. Kaduri *et al.* [19] analysed how VLMs process visual information and found that generated tokens primarily attend to query (text) embeddings rather than image embeddings. As a result, the visual information is accessed indirectly through global context encoded in query embeddings (through their interaction with image embeddings) rather than directly from the image. Tong *et al.* [16] demonstrated that some image pairs are very close in CLIP’s [24] embedding space but not in DINOv2’s [33]—a vision-only self-supervised model.

They showed that such image pairs often lead VLMs to make mistakes and proposed a new visual encoding strategy that incorporates both CLIP and DINOv2 features. Tong *et al.* [34] conducted a thorough study on what contributes to better visual representations by examining different vision encoders, connectors, training datasets, and training recipes. They also introduced a new type of connector that combines features from multiple vision encoders while incorporating an inductive spatial bias, and showed that this improves the resulting visual representations. Finally, Chen *et al.* [35] investigated why spatial reasoning is challenging for VLMs by studying the models’ attention maps. They demonstrated that smoothing the attention when the model is uncertain in its prediction and sharpening it otherwise is an effective training-free method for improving VLM performance on tasks that require spatial reasoning. However, these studies also focus on large models and do not include models with fewer than 4B parameters in their experiments.

B. VLMs in Automated Driving

Numerous studies have explored the use of VLMs in automated driving [21, 22, 36–53]. The most straightforward approach involves the use of VLMs in end-to-end driving, where it takes a traffic scene as input and outputs low-level actions. For instance, Sima *et al.* [22] decomposed the driving task into several stages, such as perception, high-level planning, and waypoint prediction, and trained a VLM to perform each step, enabling it to “control” a vehicle. Similarly, Jin *et al.* [36] trained a VLM to predict driving actions and generate textual descriptions and justifications for them. A slightly different approach was taken by Jiang *et al.* [21], who used a VLM for high-level planning in natural language. They then encoded this high-level plan and fed it, along with sensory input, into a trajectory prediction module. Their results showed that this method outperforms using only the sensory input.

Other studies have similarly investigated the application of VLMs to automated driving. Notable examples include: Choudhary *et al.* [50] combined features extracted from VLMs with Bird’s-Eye View (BEV) maps and used these augmented BEV maps as input to an LLM to analyse the visual scene. They evaluated its performance on perception, visual reasoning, and decision-making tasks. Gopalkrishnan *et al.* [51] introduced EM-VLM4AD, a lightweight VLM, and trained and evaluated it on a variety of tasks, including perception, planning, and prediction. Lübberstedt *et al.* [52] introduced V3LMA, an approach that combines LLMs and VLMs to enhance the 3D scene understanding of AI systems. This is achieved by leveraging text descriptions from object detections and video inputs alongside visual features from VLMs. Finally, Zhou *et al.* [53] addressed the problem of fine-grained information loss in the vision encoder due to downsampling while ensuring computational tractability. They proposed a novel architecture that uses a dynamic-resolution image input processing module. All these studies

train and evaluate models across a variety of tasks without focusing solely on perception capabilities.

Another line of research focuses on developing suitable benchmarks for assessing and evaluating VLMs in traffic scenarios. Marcu *et al.* [41] introduced LingoQA, a VQA benchmark for automated driving, and showed that SOTA VLMs still lag behind human performance. Xie *et al.* [44] proposed DriveBench, a benchmark for evaluating skills such as perception, prediction, and planning, and found that VLMs often produce plausible answers based on world knowledge rather than grounded visual input. Tom *et al.* [45] developed RoadTextVQA, a Video-QA benchmark focusing on reading road text and recognising traffic signs, and their evaluations revealed significant room for improvement. Chen *et al.* [46] introduced CODA-LM, a benchmark for assessing VLMs on self-driving corner cases, and tested various SOTA models. Guo *et al.* [47] presented DriveLLM, targeting spatial understanding in traffic scenes. Ding *et al.* [48] proposed NuInstruct, a challenging benchmark requiring temporal, multiview, and spatial reasoning, and introduced a method for enhancing VLMs by integrating Bird’s-Eye View (BEV) features. Finally, Charoenpitaks *et al.* [49] introduced TB-Bench, a benchmark for evaluating VLMs’ spatiotemporal understanding in traffic scenes, and their results highlighted poor performance among SOTA models. Most of these works focus on a holistic evaluation of the skills required for autonomous driving. However, this comprehensive approach makes it difficult to pinpoint specific weaknesses, as all skills are simultaneously required to solve a task. In contrast, DTPQA isolates and evaluates the perception capabilities of models in very simple visual tasks. Furthermore, DTPQA facilitates the evaluation of how these models’ perception capabilities degrade with increasing distance, an aspect crucial for traffic scenarios and, to the best of our knowledge, absent in the existing literature.

III. DTPQA

Distance-Annotated Traffic Perception Question Answering is a VQA benchmark designed to evaluate the perception-only capabilities of VLMs in traffic scenarios, using trivial yet crucial questions relevant to driving decisions. It consists of two parts: a synthetic benchmark (DTP-Synthetic) created using the CARLA simulator [54], and a real-world benchmark (DTP-Real) built on top of nuScenes [55]. Both parts are single-image VQA benchmarks aimed at assessing the perception capabilities of VLMs without requiring any reasoning skills.

A key feature of DTPQA is that it includes variations of the same question across different object distances, ranging from 5 to 50 meters, with intermediate levels at 10, 20, 30, and 40 meters. It also includes cases where the object is completely absent, referred to as *negative samples*.

In Figures 1 and 2, we can see the ten different categories of samples in DTP-Synthetic and DTP-Real. These categories were selected to satisfy two main criteria: (a)

the question must concern a simple visual concept, and (b) it must be relevant to driving decisions. For instance, knowing the direction of a walking pedestrian (category 2 in Figures 1 and 2) is crucial when planning upcoming driving actions. For example, whether a pedestrian crossing the road is moving left or right can determine whether the driver should yield or proceed, depending on the pedestrian’s position. We also included both coarse visual questions, such as the presence of a pedestrian in the scene (category 1 in Figures 1 and 2), and fine-grained ones, such as the position (left or right) of the active blinker on the vehicle ahead (category 4 in Figure 1).

In Table 1, we can get an overview of the number of samples per category and per distance in DTPQA. As shown, the number of samples across different distances is more consistent in DTP-Synthetic. This is expected, as synthetic samples can be generated on demand, whereas the same flexibility is not available for DTP-Real, which relies on images from nuScenes. A notable observation is the significantly lower number of samples in Cat.5-Synth and Cat.6-Synth. These samples involve traffic lights and signs at various distances. Their reduced sample count stems from the limited availability of such elements in CARLA. Additionally, these categories contain no samples at a 5-meter distance. At this close range, traffic lights (due to their elevation) and traffic signs (positioned on the right side of the lane) are outside the forward-facing camera’s viewing angle.

Another important feature of DTPQA is that it maintains a balanced number of samples for each possible answer at every distance. This is something that we can observe in Table 1, as the number of samples at each distance within a category is always divisible by the number of possible answers for that category. For example, as we can see in Table 1, there are 396 samples of people on either a sidewalk, crosswalk, or the road (Cat.4-Real) at a distance of 30 meters in DTP-Real. The number of possible answers in this case is 3, which divides the 396 samples into three equal parts: 132 samples with a pedestrian on a sidewalk, 132 with a pedestrian on a crosswalk, and 132 with a pedestrian on the road, all at a distance of 30 meters. The same holds true for all categories and distances. The only exception is Cat.5-Synth at 10 meters, where there are 12 samples with the answer “Red” and 11 each for “Yellow” and “Green”¹. This balance is crucial, as it prevents models from gaining an advantage based solely on language biases. For categories 1 and 3, this divisibility rule applies to the number of positive answers only, excluding the negative cases.

In the following subsections, we present a few additional details about DTP-Synthetic and DTP-Real to better understand their structure and contents.

¹We consider this slight discrepancy to be statistically insignificant and to have no meaningful impact on the evaluation of model performance for this category.

TABLE 1. Number of samples per category per distance

Distances	DTP-Synthetic							DTP-Real								
	5 m	10 m	20 m	30 m	40 m	50 m	Negative	Total	5 m	10 m	20 m	30 m	40 m	50 m	Negative	Total
Category 1	180	180	180	180	180	180	180	1260	31	303	495	660	491	401	200	2581
Category 2	180	180	180	180	180	180	-	1080	156	580	334	198	102	62	-	1432
Category 3	720	720	720	720	720	720	180	4500	45	651	1053	1056	432	162	200	3599
Category 4	270	270	270	270	270	270	-	1620	147	684	447	396	255	240	-	2169
Category 5	-	34	156	156	156	156	-	658	-	-	-	-	-	-	-	-
Category 6	-	50	50	50	50	50	-	250	-	-	-	-	-	-	-	-
Total	1350	1434	1556	1556	1556	1556	360	9368	379	1280	865	2329	2310	2218	400	9781

Cat.	Question	Example Images		Possible Answers
1	Are there any pedestrians crossing the road?			Yes No
2	In which direction is the pedestrian walking?			Left Right
3	How many pedestrians are crossing the road?			Zero One Two Three Four
4	Which of the truck's blinkers, if any, is on?			Left Right None
5	What colour is the traffic light?			Green Yellow Red
6	What is the shown traffic sign?			Speed limit (30/40/60/90) Stop

FIGURE 1. The six different categories of samples in DTP-Synthetic.

A. DTP-Synthetic

DTP-Synthetic contains 8,288 unique images of 1920x1080 resolution created using CARLA [54] and 6 different questions, resulting in a total of 9,368 unique samples (image-question pairs).

Figure 1 shows the six different categories of samples in DTP-Synthetic. As seen, the samples in DTP-Synthetic are grouped such that each unique scene is repeated multiple times, with the only variation being the distance of the object in question. In the case of static objects in categories 5 and 6 (traffic lights and signs, respectively), the ego-vehicle (and hence the camera mounted on it) must move to different

Cat.	Question	Example Images		Possible Answers
1	Are there any people in the image?			Yes No
2	In which direction is the person walking?			Left Right
3	How many people are there in the image?			Zero One Two Three
4	Where in the image is the person located?			Sidewalk Crosswalk Road

FIGURE 2. The four different categories of samples in DTP-Real.

distances from the object, resulting in slight changes in the background in these cases as well.

In Table 1, we can see the number of samples per category for DTP-Synthetic. Category 3 has overwhelmingly more samples than the rest. This is because there are multiple samples per distance in each scene to cover all the possible answers. In contrast, categories 5 and 6 have significantly fewer samples due to constraints imposed by the simulator, i.e., there is a limited number of traffic lights and signs on the maps, and only a subset can be used to maintain balance in the benchmark (e.g., having an equal number of speed limit 30 and stop signs at all distances). In Table 1, we can also see the distribution of object distances in DTP-Synthetic. As explained earlier, there are fewer samples at 5 and 10 meters because traffic lights and signs are positioned high up or at the edge of the road. The number of negative samples is much smaller, as these exist only for categories 1 and 3.

B. DTP-Real

DTP-Real contains 7,438 unique images at a resolution of 1600x900 (the native resolution of nuScenes images) and

4 different questions, resulting in a total of 9,781 unique samples. These samples were created automatically using the annotations provided by nuScenes. Figure 2 shows the 4 different categories of samples in DTP-Real.

DTP-Real differs from DTP-Synthetic in five key ways, aside from the obvious fact that it includes real images. First, by comparing Figures 1 and 2, we can see that the real part of the benchmark does not contain the exact equivalents of DTP-Synthetic scenes, as this is not possible due to missing annotations in nuScenes (e.g., traffic lights and signs). Additionally, we use the terms person/people instead of pedestrian, as the individuals present in nuScenes scenes are not always pedestrians (e.g., police officers, construction workers, etc.). Second, the traffic scenes depicted are much more cluttered and complex, being real compared to the simulated ones, which show an empty road with only the object in question. Third, the distance to the object in question is not always exact; therefore, we created six distance bins (i.e., 5m, 10m, 20m, 30m, 40m, and 50m) and assigned each sample to its nearest bin. Fourth, unlike DTP-Synthetic, DTP-Real does not include variations of the same scene across all distances, as this is not feasible with real data. Finally, there is a difference specific to category 3. In DTP-Synthetic, all pedestrians were spawned at the same distance from the vehicle with a very small perturbation, so they do not appear at the exact same point. However, for all of them, the distance from the vehicle remains nearly identical—that is, the characteristic distance of the sample. In contrast, since the samples in DTP-Real are based on real traffic scenes, we cannot expect all the people in the image (when there is more than one) to be at the same distance from the vehicle. To work around this, we define the characteristic distance of a sample as the average distance of all the people in the scene. Consequently, the variance in the distances of the people also becomes a factor influencing how difficult a sample is to answer (e.g., a sample with an average distance of 20m where one person is 5m away and another is 35m away is harder than a sample where both are at 20m), and hence we include it in the annotations of our data as well.

Despite these five differences, the main concept remains the same—i.e., each category contains multiple different samples where the object in question appears at varying distances or is completely absent (for categories 1 and 3).

In Table 1 we can see the number of samples per category in DTP-Real. The distribution is not uniform across the four categories due to the unequal availability of suitable images in nuScenes for each case. For example, category 2 requires a single pedestrian in the scene within a specific angle relative to the camera (to clearly indicate movement to the left or right), and there are fewer such images compared to category 3, which only requires multiple people in the scene. In Table 1 we can also see the number of samples per distance. As observed, samples depicting the relevant scene at very close distances (i.e., <7.5m) are less frequent by comparison.

IV. MODELS

Our goal here is to evaluate the perception capabilities of SOTA small VLMs with fewer than 4 billion parameters, as these are the models that could potentially be deployed on local hardware within a vehicle due to their smaller size. We selected the top-performing models in the <4B category from the Open VLM Leaderboard [56]. Table 2 presents the top 10 performing small VLMs on the Open VLM Leaderboard as of March 2025.

BlueLM-V-3B [57], which ranks first, is not publicly available and was therefore excluded from our experiments. The remaining models are all publicly accessible and can be readily used for inference through the Transformers API [58].

All the models listed in Table 2 follow the same high-level architecture: a Vision Encoder (typically a CLIP-like model [24]) extracts visual features from the image, a projector adjusts the dimensions of those features to match the dimension of the input space of the LLM, and a pre-trained LLM processes the concatenated visual and textual inputs. This general architecture is illustrated in Figure 3.

For most of the models in Table 2, the projector is a simple MLP. The only exceptions are the two Ovis models [59], which adopt a different approach inspired by techniques used to create text embeddings. They construct a visual embedding table (visual vocabulary \times embedding dimension), then generate a token for each visual feature by computing a probability distribution over the visual vocabulary. The final visual embedding is obtained as a weighted sum of the visual vocabulary vectors, according to this distribution.

A. Key Differences

Despite their common high-level architecture, there are some key differences in how these models process information and how they are trained. Here, we analyse these differences. It is important to note that we are excluding BlueLM-V-3B from this analysis.

The first key difference lies in how the vision encoders in these models handle images of varying resolutions. The problem arises from the fact that all vision encoders are essentially some form of Vision Transformers (ViT) [65], and therefore, can only process images of fixed size due to the fixed size of the learned positional embeddings. There are two main strategies used by the models in Table 2. The first is to avoid learned positional embeddings, in which case, there is no restriction on the resolution of images that can be processed. This is the strategy followed by Qwen2.5-VL-3B and Qwen2-VL-2B, which replace learned positional embeddings with Rotary Position Embedding (RoPE) [66]. The second strategy, used by the remaining models in Table 2, is to split the image into tiles of the desired size and process them one by one, along with a thumbnail (i.e., the entire image resized to the desired resolution) for a more holistic understanding. Aquila-VL-2B [63] and DeepSeek-

TABLE 2. Top 10 small Vision-Language Models on Open VLM Leaderboard (March 2025)

Rank	VLM	Param (B)	Language Model	Vision Encoder	Projector	Avg. Score
1	BlueLM-V-3B [57]	3.0	BlueLM-3B	SigLIP-400M	-	66.1
2	Ovis2-2B [59]	2.46	Qwen2.5-1.5B	AIMv2 Large (310M)	Linear layer + VE Table (370M)	65.2
3	Qwen2.5-VL-3B [6]	3.75	Qwen2.5-3B	QwenViT (630M)	MLP (37M)	64.5
4	SAIL-VL-2B [60]	2.1	Qwen2.5-1.5B	InternViT-300M	MLP (8.7M)	61.0
5	InternVL2.5-2B-MPO [61, 62]	2.0	InternLM2.5-1.8B	InternViT-300M-v2.5	MLP (12.6M)	60.9
6	InternVL2.5-2B [61]	2.0	InternLM2.5-1.8B	InternViT-300M-v2.5	MLP (12.6M)	59.9
7	Ovis2-1B [59]	1.27	Qwen2.5-0.5B	AIMv2 Large (310M)	Linear layer + VE Table (327M)	59.6
8	Aquila-VL-2B [63]	2.2	Qwen2.5-1.5B	SigLIP-400M	MLP (4M)	59.4
9	DeepSeek-VL2-Tiny [4]	3.4	DeepSeekMoE-3B	SigLIP-400M	MLP (7.5M)	58.1
10	Qwen2-VL-2B [64]	2.0	Qwen2-1.5B	QwenViT (630M)	MLP (34M)	57.3

The *Language Model* refers to the large language model (LLM) backbone used by each VLM. The *Vision Encoder* is the component that processes visual inputs. The *Projector* maps the visual features into the LLM's input space. The *Avg. Score* represents the average score across eight benchmark tasks (normalised to 0 - 100, the higher the better): MMBench [7], MMStar [11], MMMU [8], MathVista [9], OCRBench [12], AI2D [14], HallusionBench [13], and MMVet [10].

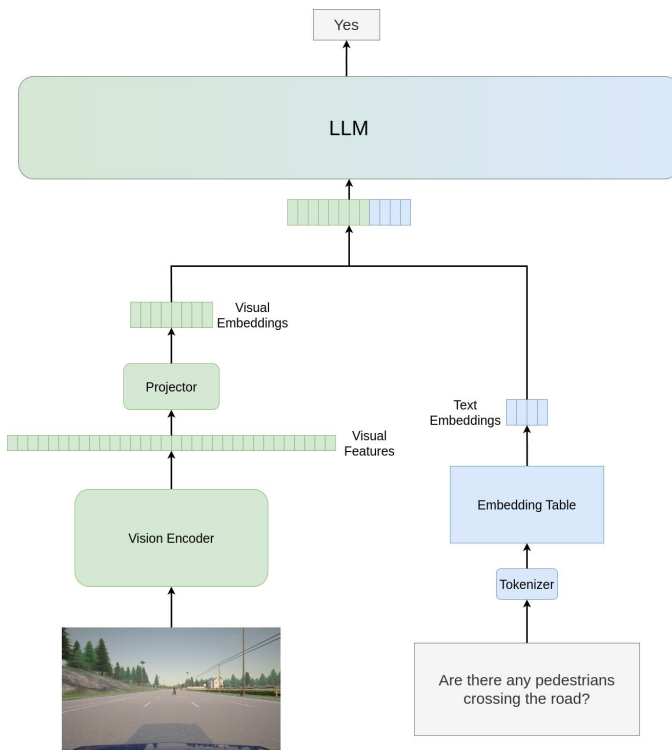


FIGURE 3. The high-level architecture that most SOTA VLMs follow.

VL2-Tiny [4] use a resolution of 384×384 for each tile, whereas the rest of the models use 448×448 .

The second key difference, already visible in Table 2, is the relative sizes of the three main components (i.e., the LLM, the vision encoder, and the projector). The optimal proportions of these components remain an open research question. In most cases, however, the vast majority of parameters are allocated to the LLM. A notable exception is Ovis2-1B, which allocates less than 50% of its parameters to its LLM backbone. As we also observe, a very small proportion of the total parameters is generally allocated to

the projector, except in the case of the two Ovis models, which allocate more than 300M parameters to the projector due to their unique approach to constructing visual embeddings. To summarise, we observe the following parameter distributions:

- Approximately 40% to 90% of the total model parameters are allocated to the LLM component (in Ovis2-1B and DeepSeek-VL2-Tiny, respectively).
- Approximately 10% to 30% is allocated to the vision encoder (in DeepSeek-VL2-Tiny and Qwen2-VL-2B, respectively).
- Approximately 0.2% to 30% is allocated to the projector (in Aquila-VL-2B and Ovis2-1B, respectively).

It is important to note here that DeepSeek-VL2-Tiny is the only model in Table 2 that uses an LLM with Mixture of Experts (MoE) layers [67]. That means that the true ratio of the computations that take place in the LLM compared to the rest of the model is much smaller than what mentioned above, as not all parameters are activated during inference for each sample.

Finally, training strategies can vary significantly, both for each component individually² and for the entire model. However, there is a common pattern followed by almost all models in Table 2, which is that training is split into multiple stages. Training begins with only the projector, or both the vision encoder and projector, and uses a large amount of relatively low-quality data. Later, the LLM is included in the training process with much higher-quality data. The only exception is InternVL2.5-2B-MPO [61, 62], which was initialized with the weights of InternVL2.5-2B [61]³ and then further trained on the Multimodal Preference dataset (MMPR) [62], a high-quality, large-scale multimodal

²The LLMs and vision encoders are typically pretrained before joint fine-tuning.

³In a sense, it still followed a staged pretraining process.

benchmark designed to enhance reasoning capabilities via chain-of-thought (CoT) prompting [68].

V. EXPERIMENTS

Here, we provide details regarding the experiments we conducted, which are divided into two categories: a) Human evaluation on DTPQA and b) VLM evaluation on DTPQA.

A. Human Evaluation

Some samples in DTPQA are difficult to answer due to the large distance of the target object, or cannot be answered at all—either because of low visibility (e.g., at nighttime, without streetlights, when a pedestrian is crossing the road 50 meters away) or due to incorrect or missing annotations in nuScenes (for DTP-Real only). Although such cases are relatively few, they lower the expected ceiling performance from 100%, despite the trivial nature of the questions in DTPQA. Therefore, we conducted a human evaluation experiment to estimate the maximum performance that can be expected from models on this benchmark.

There were 23 participants in this experiment, each answering 62 samples, i.e., one sample per category per distance for both the synthetic and real benchmarks, randomly sampled from DTPQA. For each question, the possible answers were provided in multiple-choice format. No further instructions were given to the participants. It is important to note that the relatively small number of participants imposes statistical limitations. Thus, the results of the human baseline experiment should be interpreted as indicative of the achievable performance on our dataset rather than as a definitive benchmark.

To test whether the observed differences in accuracy between humans and models were statistically significant, we performed a Monte Carlo simulation. This approach is a robust method for significance testing and is recommended when the assumptions of parametric tests may not hold, a common situation when comparing system and human performance on complex benchmarks [69]. Specifically, we estimated how likely it would be that a model, given its overall success rate across all samples, would achieve an accuracy equal to or higher than that of human participants when evaluated on a subset of samples drawn in the same way as during the human study (i.e., one sample per distance per category for all 23 participants, allowing the same sample to be selected for multiple participants). We ran 1 million simulations per model per category and considered differences non-significant if the model matched or exceeded human accuracy on the sampled subsets more than 5% of the time (one-sided $p > 0.05$).

B. VLM Evaluation

We tested models 2-10⁴ of Table 2 on DTPQA. The questions were provided to the models in multiple-choice format,

⁴As mentioned before, the weights of BlueLM-V-3B [57] are not publicly available.

and the models were explicitly prompted to respond with one of the given choices only, allowing direct comparison to the ground truth. The prompt format was as follows:

*“Strictly answer with a single word only: <question>
Possible answers: [<answers>]”*.

An exception was made for Cat.6-Synth, where the answer choices consist of more than one word (e.g., Speed limit 30). To avoid confusion, the prompt for this category was formulated as:

“<question> Choose one of the following and reply with only the answer: [<answers>]”.

This prompting strategy was effective in most cases, and the models typically restricted their responses to a single word. It is also important to note that we used greedy decoding in our experiments, as the task required the models to produce a single word (or answer), making this decoding strategy the most appropriate. However, in some instances, models generated longer responses, which made exact string comparisons insufficient for evaluating correctness.

To address this, answers were categorized as follows: an answer was considered **correct** if it matched the ground truth exactly; **unclear** if the ground truth was included in the model’s response but did not match it exactly; and **incorrect** if the ground truth was not included at all in the model’s response. Unclear samples were passed to an LLM (Qwen2.5-72B-Instruct [70]) along with the corresponding ground truth answers. The LLM labelled the VLM’s answer as either “correct” or “incorrect.” We manually reviewed a subset of these results and confirmed that Qwen2.5-72B-Instruct successfully classified the unclear samples.

In a second set of experiments, we wanted to examine the effect of slight modifications to the question on the models’ performance. To do this, we created three variants for each of the questions in Figures 1 and 2 and reran all the experiments; the variants are shown in Table 3. As we can see, in the first two variants we replaced only a single word with a synonym (italicised words in Table 3). In Variant 1, we replaced the subject of the question, while in Variant 2 we replaced the verb⁵. In contrast, in the third variant, we rephrased the entire question while maintaining its semantic equivalence to the original.

It is important to note that this is not an extensive investigation into how question phrasing affects the performance of small VLMs on simple visual questions. Our main goal is simply to assess whether minor modifications to the question can affect model performance at all, or whether the models are robust to this input noise. Additionally, we study modifications only to the main question itself, not to the prompt structure. We leave the study of the effect of prompt structure modifications on model performance for future work.

Finally, we also conducted all of the above experiments on a large SOTA VLM, namely InternVL3-78B [5], for

⁵For Cat.1-Real, “to be” was replaced with “to appear.” This could not be achieved by changing only one word, so an additional word was added.

TABLE 3. Variants of the original questions

	Variant 1	Variant 2	Variant 3
Cat.1-Synth	Are there any <i>people</i> crossing the road?	Are there any pedestrians <i>traversing</i> the road?	Do you see any pedestrians currently crossing the road?
Cat.2-Synth	In which direction is the <i>person</i> walking?	In which direction is the pedestrian <i>moving</i> ?	What direction is the pedestrian moving in?
Cat.3-Synth	How many <i>people</i> are crossing the road?	How many pedestrians are <i>traversing</i> the road?	What is the number of people crossing the road?
Cat.4-Synth	Which of the truck's <i>indicators</i> , if any, is on?	Which of the truck's blinkers, if any, is <i>activated</i> ?	Which turn indicator on the truck is active, if any?
Cat.5-Synth	What colour is the <i>stoplight</i> ?	What colour <i>shows</i> the traffic light?	What is the current colour of the traffic signal?
Cat.6-Synth	Which traffic <i>symbol</i> is shown?	Which traffic sign is <i>displayed</i> ?	What traffic sign is visible in the image?
Cat.1-Real	Are there any <i>humans</i> in the image?	Are there any people <i>appearing</i> in the image?	Do you see any humans present in the image?
Cat.2-Real	In which direction is the <i>human</i> walking?	In which direction is the person <i>moving</i> ?	What direction is the person moving toward?
Cat.3-Real	How many <i>humans</i> are in the image?	How many people <i>appear</i> in the image?	How many people can you count in the image?
Cat.4-Real	Where is the <i>human</i> located in the image?	Where is the person <i>positioned</i> in the image?	What is the person's position in the image?

comparison purposes, which at the time of this experiment ranked second on the Open VLM Leaderboard, behind only the proprietary Gemini-2.5-Pro [2].

All experiments on small VLMs were conducted on a single NVIDIA GeForce RTX 4070 Ti SUPER with 16GB of VRAM, with the only exception being DeepSeek-VL2-Tiny [4], which is incompatible with FlashAttention-2 [71] and therefore required more memory. For this reason, we used an NVIDIA A100-SXM4-40GB for this model. Finally, for the experiments involving InternVL3-78B, we utilised four NVIDIA H100 80GB HBM3 GPUs⁶.

VI. RESULTS AND ANALYSIS

In this section, we present the results of the two experiments we conducted: (i) the evaluation of the selected models on DTPQA, and (ii) the effect of slight modifications to the questions on the models' performance.

A. Performance on DTPQA

Table 4 summarises our main results, which are also visualised in Figure 4. The accuracies for each category in Table 4 are calculated as the macro-average of the accuracies across all distances. This approach compensates for the imbalance in the number of samples across distances in some categories of DTPQA. For instance, using a micro-average would make all models appear to perform much better on Cat.1-Synth than on Cat.1-Real simply because the latter contains fewer samples at 5 meters compared to other distances.

As we can see, all models, including the large InternVL3-78B, fall short of human performance in all tasks, apart from Cat.6-Synth, where multiple models appear to reach or even slightly surpass human performance. Moreover, all differences between human and model performance were confirmed to be statistically significant with an one-sided p-value less than 0.05, as determined by the Monte Carlo

⁶Four NVIDIA A100-SXM4-40GB GPUs would likely have sufficed as well, but they were unavailable at the time due to other workloads.

simulation, except for those indicated by a dagger in Table 4⁷.

Figure 4 does not capture the effect of the different chance accuracies for each task, and hence in Figure 5 we visualise the chance-corrected accuracy of the models for each task defined as:

$$a' = \begin{cases} \frac{a_o - a_c}{1 - a_c}, & \text{if } a_o > a_c \\ 0, & \text{if } a_o \leq a_c \end{cases} \quad (1)$$

where a_o is the observed accuracy and a_c is the chance accuracy. This metric reflects the proportion of samples for which the model demonstrates meaningful understanding, beyond what would be expected by random guessing. Additionally, Figure 6 illustrates the performance of the models as a function of the distance of the object in question, highlighting again the substantial gap between small VLM and human performance. Below we discuss the key findings based on the above results.

1) Strengths and Weaknesses

Here we summarise the main strengths and weaknesses of small VLMs on simple visual tasks in traffic scenes, as derived from the results.

Spatial Reasoning

As it is clearly apparent in Figure 5, some types of questions appear to be significantly more challenging for all models compared to others. In particular, questions that require distinguishing left from right seem to be the most difficult (Cat.2-Synth, Cat.4-Synth, and Cat.2-Real), even for InternVL3-78B, which performs around chance accuracy in both Cat.2-Synth and Cat.2-Real. Especially in Cat.2-Real, all models perform close to chance, whereas human performance remains high, reaching 92.0%.

This gap is further highlighted in the accuracy-by-distance results (Figure 6). As we can see, in real traffic scenes, no

⁷These exceptions occur exclusively in Cat.6-Synth, where no performance gap existed in the first place.

TABLE 4. The accuracy (%) of small VLMs in DTPQA

Method	DTP-Synthetic							DTP-Real					Avg
	Cat. 1 Presence	Cat. 2 Direction	Cat. 3 Count	Cat. 4 Blinker	Cat. 5 Light color	Cat. 6 Sign type	Avg	Cat. 1 Presence	Cat. 2 Direction	Cat. 3 Count	Cat. 4 Location	Avg	
Chance	50.0	50.0	20.0	33.3	33.3	20.0	34.4	50.0	50.0	25.0	33.3	39.6	37.0
Human Performance	95.7	97.1	81.4	80.4	93.9	82.6	88.5	82.6	92.0	74.5	74.6	80.9	84.7
InternVL3-78B	85.9	54.0	75.9	39.9	83.7	82.8 [†]	70.4	71.2	48.0	64.9	62.6	61.7	66.1
<i>Small VLMs:</i>													
Ovis2-2B	71.5	52.6	52.1	44.6	74.7	77.6 [†]	62.2	70.7	51.3	50.6	53.7	56.6	59.4
Qwen2.5-VL-3B	17.3	53.0	61.0	41.2	78.2	86.4[†]	56.2	22.9	51.6	52.8	49.3	44.2	50.2
SAIL-VL-2B	43.7	52.8	51.0	42.4	75.0	72.8	56.3	46.9	50.6	51.6	56.2	51.3	53.8
InternVL2.5-2B-MPO	71.0	55.8	54.4	36.2	80.1	74.8	62.1	68.3	49.5	51.2	57.4	56.6	59.4
InternVL2.5-2B	52.8	53.7	55.0	33.6	77.2	68.0	56.7	62.6	50.4	50.7	56.1	54.9	55.8
Ovis2-1B	33.6	48.3	39.5	33.1	77.0	51.6	47.2	63.0	49.4	39.8	43.3	48.9	48.1
Aquila-VL-2B	42.9	57.1	58.4	47.8	75.5	80.0 [†]	60.3	52.2	49.3	44.3	48.6	48.6	54.5
DeepSeek-VL2-Tiny	53.8	60.3	37.6	39.5	72.7	70.0	55.7	55.3	48.4	44.5	51.8	50.0	52.9
Qwen2-VL-2B	61.4	54.4	53.0	35.9	82.4	84.4 [†]	61.9	44.0	49.3	40.9	46.5	45.2	53.6

Accuracies shown are macro-averaged across distances, meaning they represent the average of the accuracies within each distance. The two light grey columns show macro-averages across categories, while the dark grey column represents the macro-average of the light grey columns. †The difference between model performance and human performance is not statistically significant (one-sided $p > 0.05$).

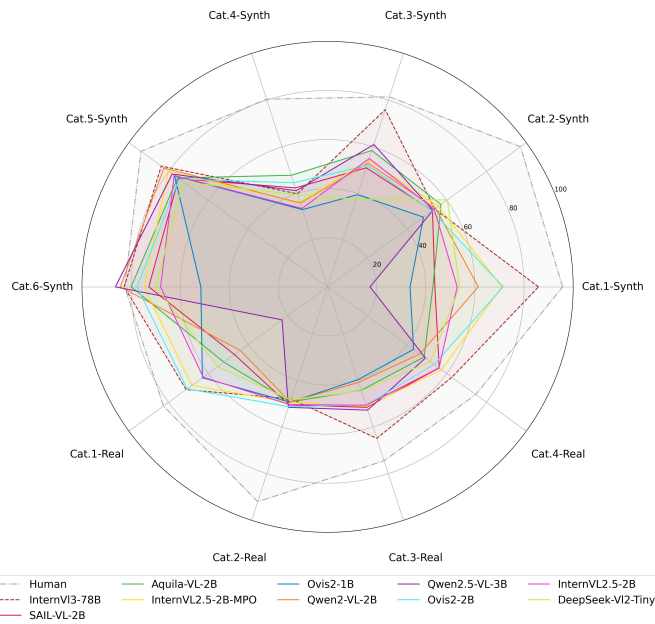


FIGURE 4. Model accuracy (%) on DTPQA.

model appears capable of identifying the direction in which a person is walking (Cat.2-Real), even when the person is only 5 meters away. In contrast, human performance on the same task is nearly perfect up to a distance of 30 meters and only slightly declines thereafter. Similarly, no model seems able to identify which indicator is on in Cat.4-Synth when the truck is 20 meters away or more, whereas human accuracy consistently remains above 60%, even at a distance of 50 meters. These results highlight the difficulty these

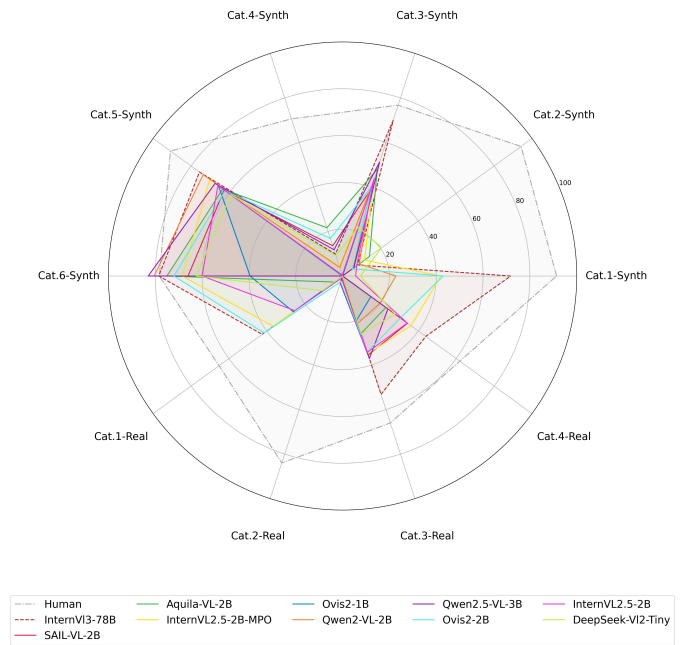


FIGURE 5. Chance-corrected accuracy (%) on DTPQA.

models have with spatial reasoning, especially with the orientation of an object.

Traffic Light and Sign Recognition

Conversely, as shown in Figure 5, most models perform very well in distinguishing colours and reading traffic signs (Cat.5-Synth and Cat.6-Synth, respectively). Based on the indicative results from the human evaluation, it appears

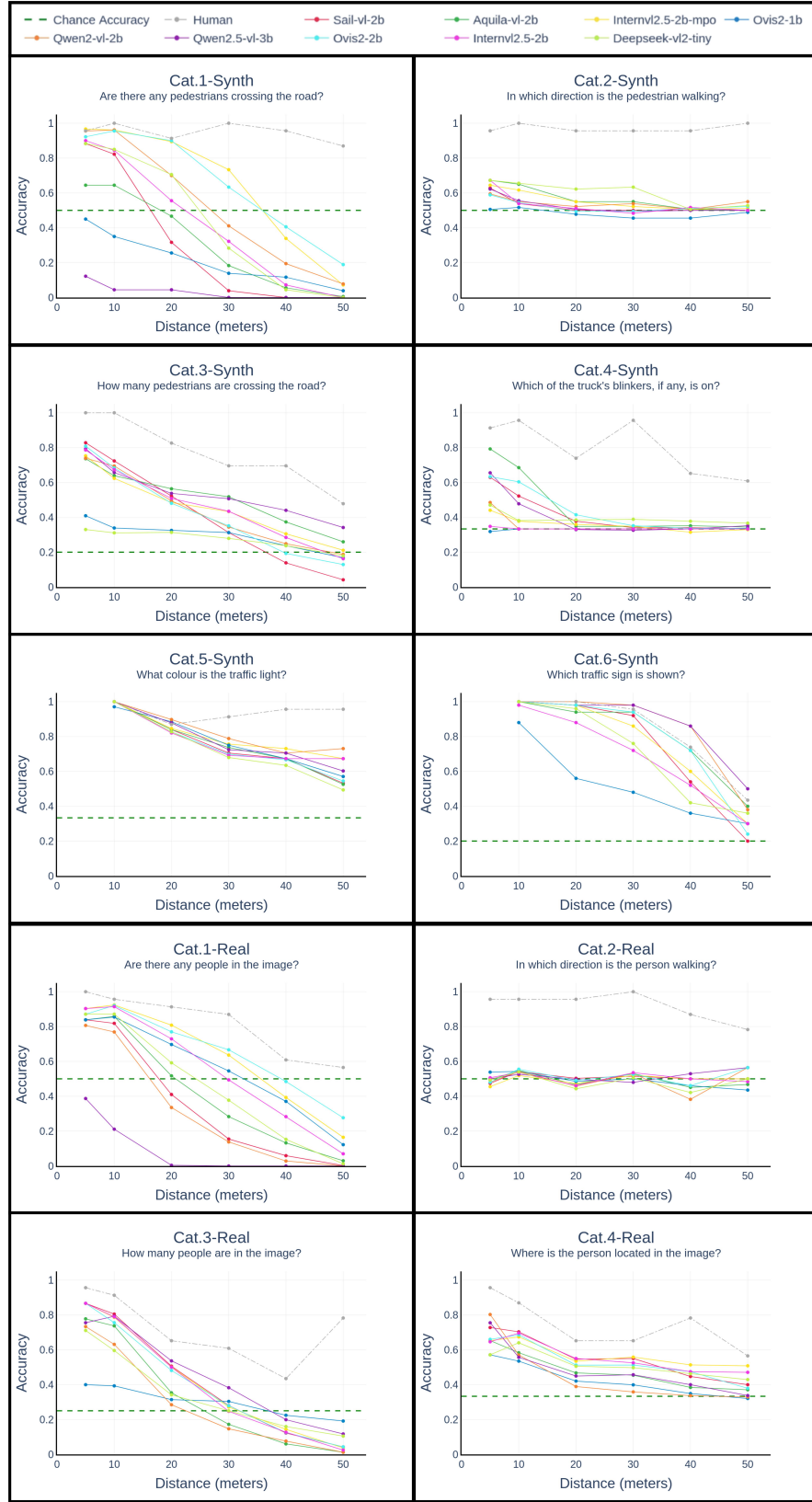


FIGURE 6. Accuracy of different VLMs across object distances for various question categories in DTPQA. Dashed green line indicates chance level.

that many small VLMs can recognize traffic signs in the scene as effectively as humans. Additionally, we can see in Figure 6 that the Qwen models seem very robust at recognising traffic signs (Cat.6-Synth) up to a distance of 30 meters, as indicated by the nearly flat performance line in the corresponding category. This may reflect strong OCR capabilities in these models.

2) Degradation of Performance with Distance

For some question types, the performance of most models drops almost linearly with distance (Cat.1-Synth, Cat.3-Synth, Cat.5-Synth, Cat.1-Real, and Cat.3-Real). At the same time, we do not observe this pattern in human performance for Cat.1-Synth and Cat.5-Synth, where accuracy remains high even at large distances. This indicates substantial room for improving the performance of small VLMs on these tasks at long distances. For Cat.3-Synth, Cat.1-Real, and Cat.3-Real, human performance also declines with increasing distance⁸, though always maintaining a large performance gap over the best small VLMs.

3) Inconsistent Model Behaviour

Looking at Qwen2.5-VL-3B in Table 4 we notice something interesting: The model seems to have performed the worst by far on Cat.1-Synth, almost always answering “No” regardless of the visual input, yet achieved the best performance on Cat.3-Synth. The same pattern was observed in the corresponding categories of DTP-Real as well. Paradoxically, the model seems capable of counting multiple pedestrians in a scene but fails to detect a single one. This highlights how the behaviour of small VLMs can sometimes be erratic and unpredictable, even when dealing with very simple visual questions. This conclusion is supported further by the results in subsection B.

4) Other Key Findings

- The results of models that share the same vision encoder but have different LLMs (e.g., Ovis2-2B and Ovis2-1B) can differ significantly. This indicates that the perception capabilities of VLMs depend not only on the vision encoder but also strongly on the LLM component. One would expect that, given a certain quality of visual features and the simple nature of the questions, performance should be similar even with different language models. However, this does not seem to be the case, suggesting that some crucial processing of the visual information itself occurs within the LLM.
- Further fine-tuning an already trained VLM on high-quality data, without changing its architecture, can sub-

stantially improve the model’s perception capabilities as is the case for InternVL2.5-2B-MPO, which has a 3.6% overall improvement compared to InternVL2.5-2B.

- Ovis2-1B and DeepSeek-VL2-Tiny seem to perform significantly worse than the other models in Cat.3-Synth. The same trend is observed for Ovis2-1B in Cat.3-Real but not for DeepSeek-VL2-Tiny. That might indicate that counting can benefit from larger language models (or more activated parameters in the LLM during inference in the case of DeepSeek-VL2-Tiny since it uses MoE layers).

5) Performance on Negative Samples

A noteworthy observation is that the only categories where model accuracy drops considerably below chance level are Cat.1-Synth, Cat.3-Synth, Cat.1-Real, and Cat.3-Real, hence the categories that include negative samples. At longer distances, when the model fails to detect the person or people in the image, it defaults to the answers of the negative samples (“No” or “Zero” for categories 1 and 3, respectively), resulting in accuracy that drops below chance. It is therefore useful to examine the models’ performance on the negative samples in these categories, which is depicted in Table 5.

As we can see, almost all models achieve close to perfect accuracy on the negative samples of DTP-Synthetic. Performance is slightly lower—but still very close to perfect—on the negative samples in DTP-Real. This could be due to: (a) the more cluttered and complex real-world traffic scenes, or (b) missing annotations in nuScenes, which may lead to some misclassified negative samples—i.e., samples containing a person but labelled as not containing any. The latter is most likely the reason for the lower human performance on the negative samples of Cat.1-Real and Cat.3-Real. More specifically, pedestrians at very long distances are often not annotated in nuScenes, even though they are visible if one looks carefully. Such cases most likely led to what appears as worse human performance on these samples. Nevertheless, the high accuracy of small VLMs on negative samples is a positive sign, suggesting a low rate of visual hallucinations for all models.

6) Failure Cases

In Figure 7, we illustrate some notable failure cases. As shown, in many instances, small VLMs appear to be “blind” even when the object in question is very close (≤ 20 m in all illustrated examples). These are questions that any human could always answer at a glance, but SOTA small VLMs still fail sometimes. This highlights once again that these models are not yet ready for use in automated driving. Regardless of their reasoning abilities, they cannot be trusted if they fail to consistently detect a pedestrian right in front of them (first

⁸An exception is the increase in accuracy from 40 to 50 meters in Cat.3-Real. We suspect this is due to noise from the relatively small number of participants in the human evaluation.

TABLE 5. Deviation from perfect accuracy (%) on negative samples.

Models	Cat.1-Synth	Cat.3-Synth	Cat.1-Real	Cat.3-Real
Human Performance	0.0	0.0	13.0	13.0
Ovis2-2B	0.0	0.0	4.0	1.0
Qwen2.5-VL-3B	0.0	0.6	0.0	9.0
SAIL-VL-2B	0.0	0.0	0.0	1.5
InternVL2.5-2B-MPO	0.0	0.6	4.5	2.5
InternVL2.5-2B	0.0	0.0	1.5	1.0
Ovis2-1B	0.0	2.8	2.0	4.0
Aquila-VL-2B	0.0	0.0	0.5	1.0
DeepSeek-VL2-Tiny	0.0	2.2	0.5	5.0
Qwen2-VL-2B	0.0	0.0	0.0	2.0

example in Figure 7) or determine which indicator light is on in the vehicle ahead (third example in Figure 7).

Overall, the above results emphasize the substantial gap between human perception and the perception systems of SOTA small VLMs in traffic scenes, and point to specific areas, such as spatial reasoning, that remain extremely challenging for these models, whereas other areas, like traffic sign recognition, match human performance.

B. Impact of Question Rephasings on Model Performance

Here, we present the results of the experiment where three variants of the original question were given to the models along with the visual input. The results, shown as deviations from the original accuracy, are presented in Table 6. Additionally, in Figures 8 and 9 we can see the performance by distance of the models for each variant. As mentioned earlier, this was not an extensive investigation into how question phrasing affects the performance of small VLMs on simple visual questions; our main goal is to assess whether minor modifications to the question can affect model performance at all. Hence, all conclusions below, beyond the main one, should be seen as indicative, based on our results. Further research is definitely needed to determine why and how changes in prompts can influence the performance of small VLMs in simple visual tasks.

1) Primary Findings

As we can see in Table 6, changes in the question can clearly affect model performance. An extreme case is that of DeepSeek-VL2-Tiny, where simply changing the question in Cat.1-Synth from “Are there any pedestrians crossing the road?” to “Do you see any pedestrians currently crossing the road?” caused a drop of 33.2 percentage points in

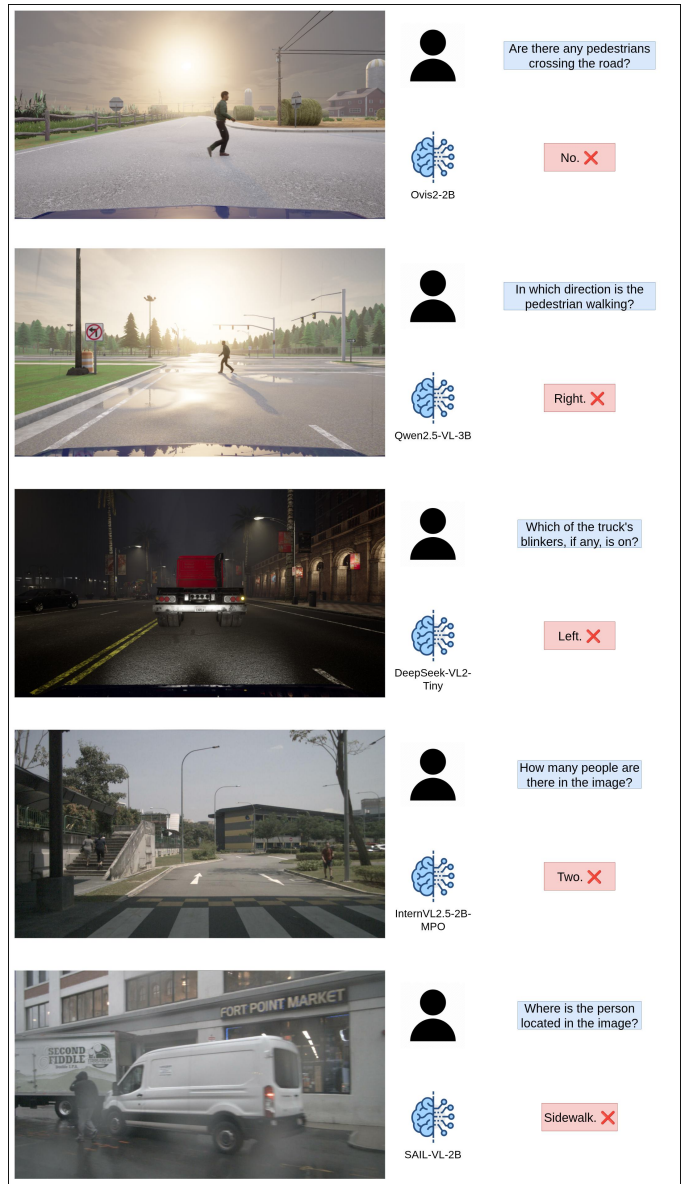


FIGURE 7. Failure cases.

accuracy. However, as becomes evident in Figures 8 and 9, and by comparing these figures with the original performance by distance (Figure 6), the overall performance patterns remain largely invariant to changes in the question. That is, models still perform much better at tasks such as identifying the colour of a traffic light or recognising a traffic sign than at determining a pedestrian’s direction or identifying which blinker is on in the vehicle ahead. We also observe the same general pattern of performance degradation with increasing distance, regardless of question phrasing. This consistency indicates that, although performance may vary across question variants, the overarching conclusions presented in subsection A remain valid.

2) Further Observations and Patterns

As we can see in Table 6, the variance in performance caused by question variants 1 and 2 is usually smaller compared to that caused by question variant 3, though not always. This may suggest a relationship between the number of words changed and the magnitude of performance variation. Furthermore, in several cases, changing only the verb has a noticeably larger effect on performance across models than changing only the subject (e.g., Cat.1-Synth, Cat.2-Synth, Cat.3-Synth), whereas the reverse occurs only once (Cat.1-Real). This may indicate a stronger model reliance on verb choice than on other parts of speech.

Another notable finding is that the effect of changing the question is much stronger for some types of questions than others. For example, we see that changing the question for Cat.1-Synth has a significant impact on the performance of most models (for both variants), whereas it has little effect in other categories (Cat.5-Synth, Cat.2-Real, Cat.4-Real). A possible explanation for this could be that in the case of Cat.2-Real the visual information is lost at some point, so changing the prompt can't have any major impact on the performance, as this was already at chance level. Regarding Cat.5-Synth it might be the exact opposite, i.e., the visual information about the colour of the traffic light is very well encoded within the visual embeddings and hence simple changes in the prompt can't make a big difference.

We also observe that the same change in a question can produce very different effects across models. For example, the second variant in Cat.1-Synth leads to an increase in accuracy of 21.0 percentage points for Ovis2-1B but a decrease of 33.2 points for DeepSeek-VL2-Tiny, indicating that models do not respond uniformly to identical prompt changes. Nonetheless, there are interesting exceptions: the second variant of the question for both Cat.1-Synth and Cat.3-Synth consistently improves performance across all models. Notably, both apply the same modification, namely replacing “crossing” with “traversing”. This suggests that small VLMs may align the visual features that encode a pedestrian crossing the road (or, in the case of Cat.3-Synth, the number of pedestrians) more strongly with the embedding of “traversing” than with that of “crossing.” Similarly, replacing “traffic light” with “stoplight” in Cat.5-Synth slightly degrades performance across all models. Finally, variant 3 of Cat.1-Synth reduces performance for almost all models (Ovis2-1B being the sole exception), often substantially. This question differs in two respects: (a) the “Do you see” format and (b) the inclusion of the word “currently.” Because variant 3 of Cat.1-Real, which also uses “Do you see” but not “currently,” mostly improves performance, the negative effect appears more likely driven by “currently,” which may bias models toward answering “No” regardless of the visual input.

The overall effect of identical changes can also differ widely between models. The average change in accuracy across all tasks ranges from 1.9 to 5.0 absolute percentage

points for different models. Additionally, the results show that a much larger model size appears to mitigate but not solve this negative effect, as InternVL3-78B shows a smaller average change in accuracy of only 1.3 percentage points.

Finally, Table 7 presents the models’ performance, as deviation from perfect accuracy, on the negative samples of DTPQA for all variant groups. As we can see, in most cases, performance remains close to perfect, as in the original experiment. However, there are also cases where performance drops substantially—for instance, Qwen2.5-VL-3B in Cat.3-Real when given the question variant 3. This drop helps explain the above-chance accuracy observed for this model in Cat.3-Real in Figure 9 (Variant 3), even at 50 meters. The model simply answered “Zero” much less often, increasing the chance of being correct when people were present in the scene from 1 out of 4 to 1 out of 3 (33.3%), which matches the performance observed in Figure 9.

Overall, the fact that the performance of small VLMs can be affected, even in individual cases, by question rephrasing suggests that performance depends not only on whether the visual information required to answer the question is available (i.e., encoded in the visual embeddings), but also on how this information interacts with the text embeddings of the chosen question, even when the questions are semantically equivalent. This is clearly a concerning result for safety-critical applications, as we do not want our systems to fail simply because the task was phrased differently.

VII. LIMITATIONS AND FUTURE SCOPE

In this work, we quantitatively measured the strength of the perception systems of small SOTA VLMs in traffic scenes and identified specific cases where these models are particularly weak. However, we did not address the question of **why** these models fail in these particular cases or how they could be improved. The wide range of components that influence a VLM’s perception capabilities (LLM backbone, vision encoder, projector, training strategies, training datasets, etc.) makes it extremely difficult to determine which factors are responsible for strong or weak performance. Future work could involve a mechanistic interpretability approach, where we closely examine how visual information is processed within each component of the model for each of these tasks and identify where it is “lost” in failure cases. Specifically, techniques such as attention visualization, probing experiments, and activation patching could be used to determine how visual information flows through the model. Based on the insights that will be gained from this analysis, we could then attempt to enhance the perception capabilities of small VLMs in traffic scenes without compromising their performance on other tasks. Additionally, another promising direction for future work is a more comprehensive investigation of the prompt sensitivity of these models in simple visual tasks. This could involve studying a broader range of question variations as well as exploring different prompt structures—an aspect that was not examined in this study.

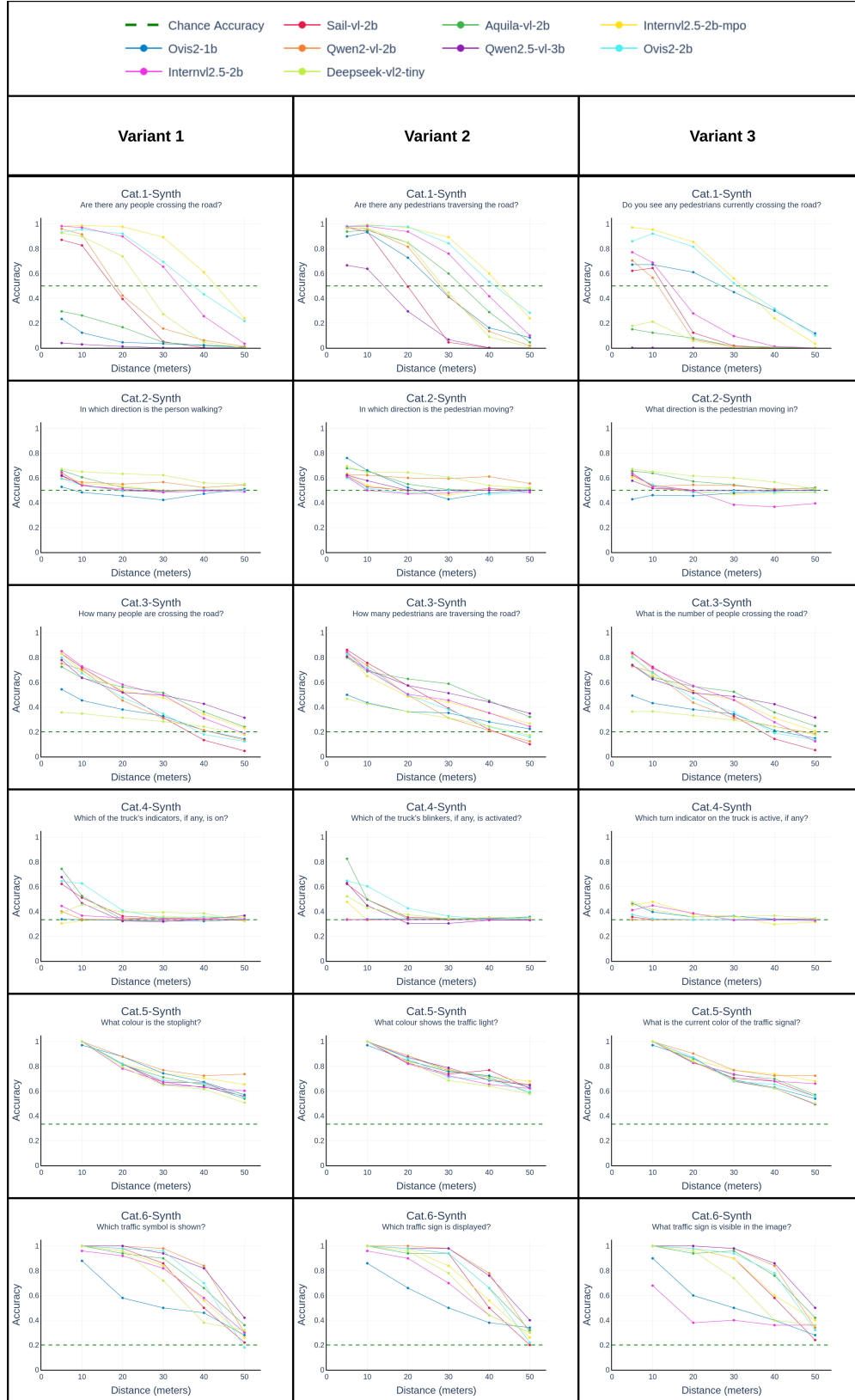


FIGURE 8. Performance by distance on DTP-Synthetic for all question variations.

TABLE 6. Deviation from original accuracy (%) for each question variant and model.

Method	DTP-Synthetic																		DTP-Real								Avg				
	Cat. 1 Presence			Cat. 2 Direction			Cat. 3 Count			Cat. 4 Blinker			Cat. 5 Light color			Cat. 6 Sign type			Cat. 1 Presence		Cat. 2 Direction		Cat. 3 Count		Cat. 4 Location						
	Var.1	Var.2	Var.3	Var.1	Var.2	Var.3	Var.1	Var.2	Var.3	Var.1	Var.2	Var.3	Var.1	Var.2	Var.3	Var.1	Var.2	Var.3	Var.1	Var.2	Var.1	Var.2	Var.1	Var.2	Var.1	Var.2		Var.3			
InternVL3-78B	1.7	3.5	8.4	0.3	0.1	1.1	0.1	1.4	0.1	1.6	0.8	1.5	3.3	0.4	1.4	0.4	0.4	0.8	0.8	1.6	3.0	1.5	0.6	0.3	0.0	0.1	1.3	0.7	0.5	1.0	1.3
<i>Small VLMs:</i>																															
Ovis2-2B	2.2	8.7	6.7	0.6	1.9	0.5	0.7	2.5	0.2	0.8	0.6	10.5	0.3	2.6	0.6	1.2	1.6	2.8	0.7	0.1	1.0	0.3	0.2	1.2	1.1	3.1	4.5	1.6	1.7	3.3	2.1
Qwen2.5-VL-3B	1.9	20.8	3.0	0.5	0.3	1.4	1.4	1.5	2.4	0.3	2.1	6.9	4.9	1.7	4.9	2.8	4.0	0.4	10.6	1.2	8.7	2.3	1.3	1.5	3.0	1.0	1.5	0.4	0.9	1.9	3.2
SAIL-VL-2B	1.2	5.6	9.3	0.1	0.4	0.1	0.1	4.7	0.6	0.6	1.0	8.7	0.8	4.1	0.5	1.6	0.4	1.2	1.4	1.4	3.1	0.3	0.1	0.2	0.2	2.4	0.4	1.5	0.8	3.2	1.9
InternVL2.5-2B-MPO	10.3	10.2	5.0	1.9	3.1	5.2	4.1	2.8	2.2	2.4	0.3	1.8	1.6	0.0	0.7	2.4	2.0	2.8	5.4	4.8	11.8	0.5	0.5	1.2	0.5	1.9	3.1	1.7	1.1	3.8	3.2
InternVL2.5-2B	15.8	21.2	12.2	1.0	2.7	6.9	4.3	3.4	1.9	2.6	0.3	3.6	3.5	0.8	0.9	3.6	2.0	24.4	5.2	4.4	13.0	1.4	2.1	0.4	2.4	0.7	2.6	1.0	0.9	3.8	5.0
Ovis2-1B	12.7	26.6	21.0	0.4	7.5	1.3	4.2	5.5	3.5	0.1	1.0	4.4	0.3	1.5	3.1	2.4	3.2	2.0	0.6	1.8	5.4	2.5	1.5	1.1	3.5	8.3	4.0	0.5	1.8	0.2	4.4
Aquila-VL-2B	17.3	23.8	23.4	2.2	0.4	0.2	0.7	5.6	0.2	3.5	3.0	14.5	1.3	3.3	1.2	2.8	2.8	1.6	1.1	2.1	1.0	1.2	1.2	1.7	1.6	4.1	2.1	2.9	1.9	9.1	4.6
DeepSeek-VL2-Tiny	1.7	7.9	33.2	1.2	0.4	0.0	1.0	5.0	1.9	0.5	0.1	0.9	1.4	2.2	0.2	2.4	0.4	0.8	3.8	3.2	2.7	1.3	0.1	3.3	1.7	0.3	2.8	0.4	0.7	0.1	2.7
Qwen2-VL-2B	11.0	0.3	27.8	1.3	5.8	0.2	2.1	0.1	1.8	1.4	2.5	2.6	0.2	2.3	0.0	2.0	3.2	1.2	6.9	0.1	3.1	0.1	0.1	3.2	0.4	1.5	2.3	0.5	1.2	1.0	2.9
Average	8.2	13.9	15.7	1.0	2.5	1.8	2.1	3.5	1.6	1.4	1.2	6.0	1.6	2.1	1.3	2.4	2.2	4.1	4.0	2.1	5.5	1.1	0.8	1.5	1.6	2.6	2.6	1.2	1.2	2.9	

Green indicates increased accuracy compared to the original performance, while red indicates decreased accuracy. The average change in accuracy for each category was calculated based only on the small VLMs.

TABLE 7. Deviation from perfect accuracy (%) on negative samples for question variants 1, 2, and 3.

Models	Var.1				Var.2				Var.3			
	Cat.1-Synth	Cat.3-Synth	Cat.1-Real	Cat.3-Real	Cat.1-Synth	Cat.3-Synth	Cat.1-Real	Cat.3-Real	Cat.1-Synth	Cat.3-Synth	Cat.1-Real	Cat.3-Real
Ovis2-2B	0.0	0.0	3.0	0.0	0.0	0.0	5.0	3.5	0.0	0.0	3.5	4.0
Qwen2.5-VL-3B	0.0	0.0	0.0	9.5	0.0	1.1	0.0	6.5	0.0	0.6	0.0	52.0
SAIL-VL-2B	0.0	0.0	0.0	1.0	0.0	0.0	0.0	3.0	0.0	0.0	0.0	2.5
InternVL2.5-2B-MPO	0.0	0.6	8.5	2.5	0.0	1.7	2.0	2.0	0.0	1.1	47.5	2.0
InternVL2.5-2B	0.0	0.0	3.5	1.5	0.0	1.1	0.5	1.5	0.0	0.0	18.5	0.5
Ovis2-1B	0.0	0.0	1.0	12.5	0.0	0.6	2.0	6.5	0.0	0.0	2.0	6.5
Aquila-VL-2B	0.0	0.0	0.5	1.0	0.0	0.0	1.0	3.0	0.0	0.0	0.5	2.5
DeepSeek-VL2-Tiny	0.0	2.2	2.0	6.0	0.0	0.6	0.0	5.5	0.0	1.1	0.0	6.0
Qwen2-VL-2B	0.0	0.0	0.0	2.0	0.0	0.0	0.0	1.0	0.0	0.0	0.0	1.5

VIII. CONCLUSION

In this paper, we evaluate the perception capabilities of SOTA small VLMs in traffic scenes as a function of the distance of the object in question. To do so, we introduce DTPQA, a novel VQA benchmark with both synthetic and real images. Our results show that the perception capabilities of SOTA small VLMs remain very weak, especially in specific areas such as distinguishing left from right, and are far from being trustworthy in safety-critical applications. Additionally, we show that small VLMs tend to be very shortsighted, as their perception capabilities degrade further with increasing distance, even in cases where human perception does not exhibit the same pattern, making them even less suitable for automated driving, where many critical objects are distant. Finally, we demonstrate that simply rephrasing a question can lead to significant performance changes in specific cases. However, the overall performance patterns remain consistent, confirming that some visual concepts are inherently more difficult for these models to grasp, regardless of how the question is phrased. Our results reveal specific weaknesses of modern small VLMs in traffic scenes; however, further research is needed to determine the exact causes of these failures and ultimately to improve the perception capabilities of these models, which could be valuable for deployment in hardware-constrained applications.

IX. ETHICS STATEMENT

The informed consent required for participation in this study was duly obtained from all subjects involved in the data collection process. This research adheres to the principles set forth in the Declaration of Helsinki and received ethical approval from the University of Limerick’s Ethics Committee (protocol/approval number: 2025_06_04_S&E).

The research team acknowledges the participants’ right to privacy and protection from undue exposure regarding their personal lives. To safeguard these rights, all participants were fully briefed on the objectives of the study. Furthermore, the anonymity of each participant’s data has been rigorously maintained.

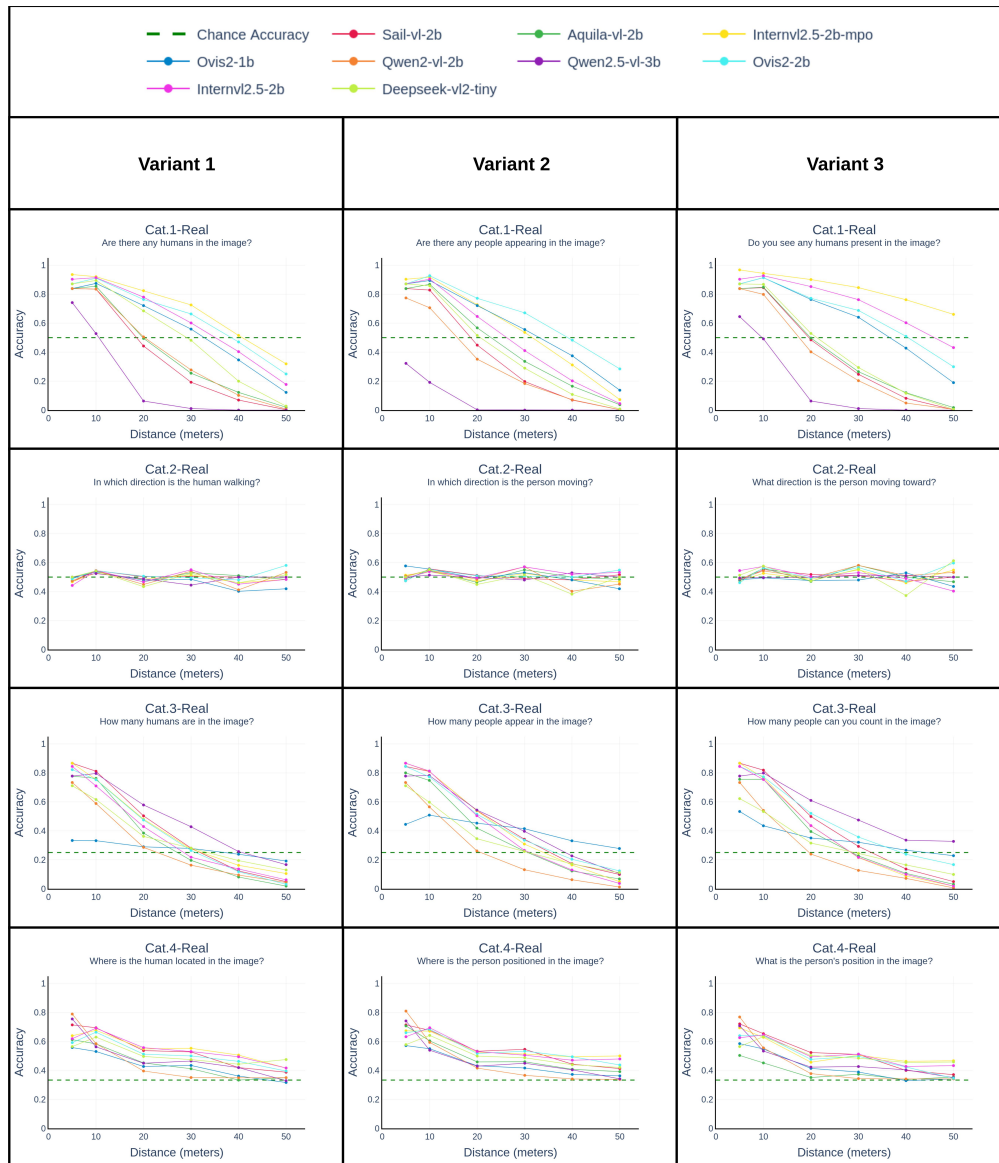


FIGURE 9. Performance by distance on DTP-Real for all question variations.

REFERENCES

[1] OpenAI, “Gpt-4o: Openai’s new flagship model,” <https://openai.com/index/gpt-4o>, May 2024, openAI Blog. [Online]. Available: <https://openai.com/index/hello-gpt-4o/>

[2] K. Kavukcuoglu, “Gemini 2.5: Our most intelligent ai model,” <https://blog.google/technology/google-deepmind/gemini-model-thinking-updates-march-2025/#gemini-2-5-thinking>, March 2025, google Blog. [Online]. Available: <https://blog.google/technology/google-deepmind/gemini-model-thinking-updates-march-2025/#gemini-2-5-thinking>

[3] Anthropic, “Claude 3.7 sonnet and claude code,” <https://www.anthropic.com/news/claude-3-7-sonnet>, February 2025, anthropic Blog. [Online]. Available: <https://www.anthropic.com/news/claude-3-7-sonnet>

[4] Z. Wu, X. Chen, Z. Pan, X. Liu, W. Liu, D. Dai, H. Gao, Y. Ma, C. Wu, B. Wang, Z. Xie, Y. Wu, K. Hu, J. Wang, Y. Sun, Y. Li, Y. Piao, K. Guan, A. Liu, X. Xie, Y. You, K. Dong, X. Yu, H. Zhang, L. Zhao, Y. Wang, and C. Ruan, “Deepseek-vl2: Mixture-of-experts vision-language models for advanced multimodal understanding,” 12 2024. [Online]. Available: <http://arxiv.org/abs/2412.10302>

[5] J. Zhu, W. Wang, Z. Chen, Z. Liu, S. Ye, L. Gu, H. Tian, Y. Duan, W. Su, J. Shao, Z. Gao, E. Cui, X. Wang, Y. Cao, Y. Liu, X. Wei, H. Zhang, H. Wang, W. Xu, H. Li, J. Wang, N. Deng, S. Li, Y. He, T. Jiang, J. Luo, Y. Wang, C. He, B. Shi, X. Zhang, W. Shao, J. He, Y. Xiong, W. Qu, P. Sun,

- P. Jiao, H. Lv, L. Wu, K. Zhang, H. Deng, J. Ge, K. Chen, L. Wang, M. Dou, L. Lu, X. Zhu, T. Lu, D. Lin, Y. Qiao, J. Dai, and W. Wang, "Internvl3: Exploring advanced training and test-time recipes for open-source multimodal models," 4 2025. [Online]. Available: <http://arxiv.org/abs/2504.10479>
- [6] S. Bai, K. Chen, X. Liu, J. Wang, W. Ge, S. Song, K. Dang, P. Wang, S. Wang, J. Tang, H. Zhong, Y. Zhu, M. Yang, Z. Li, J. Wan, P. Wang, W. Ding, Z. Fu, Y. Xu, J. Ye, X. Zhang, T. Xie, Z. Cheng, H. Zhang, Z. Yang, H. Xu, and J. Lin, "Qwen2.5-vl technical report," 2 2025. [Online]. Available: <http://arxiv.org/abs/2502.13923>
- [7] Y. Liu, H. Duan, Y. Zhang, B. Li, S. Zhang, W. Zhao, Y. Yuan, J. Wang, C. He, Z. Liu, K. Chen, and D. Lin, "Mmbench: Is your multi-modal model an all-around player?" in *European conference on computer vision*, 7 2023, pp. 216–233. [Online]. Available: <http://arxiv.org/abs/2307.06281>
- [8] X. Yue, Y. Ni, T. Zheng, K. Zhang, R. Liu, G. Zhang, S. Stevens, D. Jiang, W. Ren, Y. Sun, C. Wei, B. Yu, R. Yuan, R. Sun, M. Yin, B. Zheng, Z. Yang, Y. Liu, W. Huang, H. Sun, Y. Su, and W. Chen, "Mmmu: A massive multi-discipline multimodal understanding and reasoning benchmark for expert agi," in *2024 IEEE/CVF Conference on Computer Vision and Pattern Recognition (CVPR)*. IEEE, 6 2024, pp. 9556–9567. [Online]. Available: <https://ieeexplore.ieee.org/document/10656299/>
- [9] P. Lu, H. Bansal, T. Xia, J. Liu, C. Li, H. Hajishirzi, H. Cheng, K.-W. Chang, M. Galley, and J. Gao, "Mathvista: Evaluating mathematical reasoning of foundation models in visual contexts," in *The Twelfth International Conference on Learning Representations*, 2024.
- [10] W. Yu, Z. Yang, L. Li, J. Wang, K. Lin, Z. Liu, X. Wang, and L. Wang, "Mm-vet: Evaluating large multimodal models for integrated capabilities," in *Proceedings of the 41st International Conference on Machine Learning*, 2024.
- [11] L. Chen, J. Li, X. Dong, P. Zhang, Y. Zang, Z. Chen, H. Duan, J. Wang, Y. Qiao, D. Lin, and F. Zhao, "Are we on the right way for evaluating large vision-language models?" in *Advances in Neural Information Processing Systems*, 2024, pp. 27 056–27 087.
- [12] Y. Liu, Z. Li, M. Huang, B. Yang, W. Yu, C. Li, X. Yin, C. lin Liu, L. Jin, and X. Bai, "Ocrbench: On the hidden mystery of ocr in large multimodal models," 5 2023.
- [13] T. Guan, F. Liu, X. Wu, R. Xian, Z. Li, X. Liu, X. Wang, L. Chen, F. Huang, Y. Yacoob, D. Manocha, and T. Zhou, "Hallusionbench: An advanced diagnostic suite for entangled language hallucination and visual illusion in large vision-language models," in *Proceedings of the IEEE/CVF Conference on Computer Vision and Pattern Recognition*, 2024, pp. 14 375–14 385.
- [14] A. Kembhavi, M. Salvato, E. Kolve, M. Seo, H. Hajishirzi, and A. Farhadi, "A diagram is worth a dozen images," in *Computer Vision—ECCV 2016: 14th European Conference*, 2016, pp. 235–251.
- [15] P. Rahmzadehgervi, L. Bolton, M. R. Taesiri, and A. T. Nguyen, "Vision language models are blind," in *Proceedings of the Asian Conference on Computer Vision*, 7 2024, pp. 18–34. [Online]. Available: <http://arxiv.org/abs/2407.06581>
- [16] S. Tong, Z. Liu, Y. Zhai, Y. Ma, Y. LeCun, and S. Xie, "Eyes wide shut? exploring the visual shortcomings of multimodal llms," in *2024 IEEE/CVF Conference on Computer Vision and Pattern Recognition (CVPR)*. IEEE, 6 2024, pp. 9568–9578. [Online]. Available: <https://ieeexplore.ieee.org/document/10655378/>
- [17] C. Gou, A. Felemban, F. F. Khan, D. Zhu, J. Cai, H. Rezafofighi, and M. Elhoseiny, "How well can vision language models see image details?" 8 2024. [Online]. Available: <http://arxiv.org/abs/2408.03940>
- [18] R. Kamoi, Y. Zhang, S. S. S. Das, R. H. Zhang, and R. Zhang, "Visonlyqa: Large vision language models still struggle with visual perception of geometric information," 12 2024. [Online]. Available: <http://arxiv.org/abs/2412.00947>
- [19] O. Kaduri, S. Bagon, and T. Dekel, "What's in the image? a deep-dive into the vision of vision language models," in *Proceedings of the Computer Vision and Pattern Recognition Conference*, 11 2025, pp. 14 549–14 558. [Online]. Available: <http://arxiv.org/abs/2411.17491>
- [20] S. Sharma, A. Das, G. Sistu, M. Halton, and C. Eising, "Mmtrap: Multi-sensor multi-agent trajectory prediction in bev," *IEEE Open Journal of Vehicular Technology*, vol. 6, pp. 1551–1567, 2025.
- [21] B. Jiang, S. Chen, B. Liao, X. Zhang, W. Yin, Q. Zhang, C. Huang, W. Liu, and X. Wang, "Senna: Bridging large vision-language models and end-to-end autonomous driving," 10 2024. [Online]. Available: <http://arxiv.org/abs/2410.22313>
- [22] C. Sima, K. Renz, K. Chitta, L. Chen, H. Zhang, C. Xie, P. Luo, A. Geiger, and H. Li, "Drivelm: Driving with graph visual question answering," in *European Conference on Computer Vision*, 12 2024, pp. 256–274. [Online]. Available: <http://arxiv.org/abs/2312.14150>
- [23] NVIDIA, "Nvidia jetson orin," NVIDIA Documentation, November 2021. [Online]. Available: <https://www.nvidia.com/en-us/autonomous-machines/embedded-systems/jetson-orin/>
- [24] A. Radford, J. W. Kim, C. Hallacy, A. Ramesh, G. Goh, S. Agarwal, G. Sastry, A. Askell, P. Mishkin, J. Clark, G. Krueger, and I. Sutskever, "Learning transferable visual models from natural language supervision," in *International conference on machine learning*, 2 2021, pp. 8748–8763. [Online]. Available: <http://arxiv.org/abs/2103.00020>

- [25] H. Liu, C. Li, Q. Wu, and Y. J. Lee, “Visual instruction tuning,” *Advances in neural information processing systems*, vol. 36, 4 2023. [Online]. Available: <http://arxiv.org/abs/2304.08485>
- [26] J. B. Alayrac, J. Donahue, P. Luc, A. Miech, I. Barr, Y. Hasson, K. Lenc, A. Mensch, K. Millican, M. Reynolds, R. Ring, E. Rutherford, S. Cabi, T. Han, Z. Gong, S. Samangooei, M. Monteiro, J. Menick, S. Borgeaud, A. Brock, A. Nematzadeh, S. Sharifzadeh, M. Binkowski, R. Barreira, O. Vinyals, A. Zisserman, and K. Simonyan, “Flamingo: a visual language model for few-shot learning,” *Advances in neural information processing systems*, vol. 35, pp. 23 716–23 756, 2022.
- [27] Z. Chen, J. Wu, W. Wang, W. Su, G. Chen, S. Xing, M. Zhong, Q. Zhang, X. Zhu, L. Lu, B. Li, P. Luo, T. Lu, Y. Qiao, and J. Dai, “Internvl: Scaling up vision foundation models and aligning for generic visual-linguistic tasks,” in *Proceedings of the IEEE/CVF Conference on Computer Vision and Pattern Recognition*, 2024, pp. 24 185–24 198. [Online]. Available: <https://arxiv.org/abs/2312.14238>
- [28] J. Bai, S. Bai, S. Yang, S. Wang, S. Tan, P. Wang, J. Lin, C. Zhou, and J. Zhou, “Qwen-vl: A versatile vision-language model for understanding, localization, text reading, and beyond,” 8 2023. [Online]. Available: <http://arxiv.org/abs/2308.12966>
- [29] H. Lu, W. Liu, B. Zhang, B. Wang, K. Dong, B. Liu, J. Sun, T. Ren, Z. Li, H. Yang, Y. Sun, C. Deng, H. Xu, Z. Xie, and C. Ruan, “Deepseek-vl: Towards real-world vision-language understanding,” 3 2024. [Online]. Available: <http://arxiv.org/abs/2403.05525>
- [30] Anthropic, “Introducing claude 3.5 sonnet,” <https://www.anthropic.com/news/claude-3-5-sonnet>, June 2024, anthropic Blog. [Online]. Available: <https://www.anthropic.com/news/claude-3-5-sonnet>
- [31] D. H. Sundar Pichai, “Our next-generation model: Gemini 1.5,” <https://blog.google/technology/ai/google-gemini-next-generation-model-february-2024/#sundar-note>, February 2024, google Blog. [Online]. Available: <https://blog.google/technology/ai/google-gemini-next-generation-model-february-2024/#sundar-note>
- [32] —, “Internvl2: Better than the best—expanding performance boundaries of open-source multimodal models with the progressive scaling strategy,” <https://internvl.github.io/blog/2024-07-02-InternVL-2.0/>, July 2024. [Online]. Available: <https://internvl.github.io/blog/2024-07-02-InternVL-2.0/>
- [33] M. Oquab, T. Darcet, T. Moutakanni, H. Vo, M. Szafraniec, V. Khalidov, P. Fernandez, D. Haziza, F. Massa, A. El-Nouby, M. Assran, N. Ballas, W. Galuba, R. Howes, P.-Y. Huang, S.-W. Li, I. Misra, M. Rabbat, V. Sharma, G. Synnaeve, H. Xu, H. Jegou, J. Mairal, P. Labatut, A. Joulin, and P. Bojanowski, “Dinov2: Learning robust visual features without supervision,” *Transactions on Machine Learning Research*, 4 2024. [Online]. Available: <http://arxiv.org/abs/2304.07193>
- [34] S. Tong, E. Brown, P. Wu, S. Woo, M. Middepogu, S. C. Akula, J. Yang, S. Yang, A. Iyer, X. Pan, A. Wang, R. Fergus, Y. LeCun, and S. Xie, “Cambrian-1: A fully open, vision-centric exploration of multimodal llms,” *Advances in Neural Information Processing Systems*, vol. 37, pp. 87 310–87 356, 6 2024. [Online]. Available: <http://arxiv.org/abs/2406.16860>
- [35] S. Chen, T. Zhu, R. Zhou, J. Zhang, S. Gao, J. C. Niebles, M. Geva, J. He, J. Wu, and M. Li, “Why is spatial reasoning hard for vlms? an attention mechanism perspective on focus areas,” in *Forty-second International Conference on Machine Learning*, 3 2025. [Online]. Available: <http://arxiv.org/abs/2503.01773>
- [36] B. Jin, X. Liu, Y. Zheng, P. Li, H. Zhao, T. Zhang, Y. Zheng, G. Zhou, and J. Liu, “Adapt: Action-aware driving caption transformer,” in *Proceedings - IEEE International Conference on Robotics and Automation*, vol. 2023-May. Institute of Electrical and Electronics Engineers Inc., 2023, pp. 7554–7561.
- [37] P. Zheng, Y. Zhao, Z. Gong, H. Zhu, and S. Wu, “Simplellm4ad: An end-to-end vision-language model with graph visual question answering for autonomous driving,” 7 2024. [Online]. Available: <http://arxiv.org/abs/2407.21293>
- [38] S. Jiao and Y. Fang, “Lavida drive: Vision-text interaction vlm for autonomous driving with token selection, recovery and enhancement,” 11 2024. [Online]. Available: <http://arxiv.org/abs/2411.12980>
- [39] S. Wang, Z. Yu, X. Jiang, S. Lan, M. Shi, N. Chang, J. Kautz, Y. Li, and J. M. Alvarez, “Omnidrive: A holistic llm-agent framework for autonomous driving with 3d perception, reasoning and planning,” 5 2024. [Online]. Available: <http://arxiv.org/abs/2405.01533>
- [40] X. Zhou, K. Larintzakis, H. Guo, W. Zimmer, M. Liu, H. Cao, J. Zhang, V. Lakshminarasimhan, L. Strand, and A. C. Knoll, “Tumtraffic-videoqa: A benchmark for unified spatio-temporal video understanding in traffic scenes,” in *Forty-second International Conference on Machine Learning*, 2025. [Online]. Available: <http://trafix-videoqa.github.io>
- [41] A.-M. Marcu, L. Chen, J. Hünemann, A. Karnsund, B. Hanotte, P. Chidananda, S. Nair, V. Badrinarayanan, A. Kendall, J. Shotton, E. Arani, and O. Sinavski, “Lingoqa: Visual question answering for autonomous driving,” in *European Conference on Computer Vision*, 12 2024, pp. 252–269. [Online]. Available: <http://arxiv.org/abs/2312.14115>
- [42] J. Lübberstedt, E. Rivera, N. Uhlemann, and M. Lienkamp, “V3lma: Visual 3d-enhanced language model for autonomous driving,” in *Proceedings of the Computer Vision and Pattern Recognition*

- Conference*, 2025, pp. 4769–4778. [Online]. Available: <http://arxiv.org/abs/2505.00156>
- [43] Z. Qiao, H. Li, Z. Cao, and H. X. Liu, “Lightemma: Lightweight end-to-end multimodal model for autonomous driving,” 2025. [Online]. Available: <http://arxiv.org/abs/2505.00284>
- [44] S. Xie, L. Kong, Y. Dong, C. Sima, W. Zhang, Q. A. Chen, Z. Liu, and L. Pan, “Are vlms ready for autonomous driving? an empirical study from the reliability, data, and metric perspectives,” 1 2025. [Online]. Available: <http://arxiv.org/abs/2501.04003>
- [45] G. Tom, M. Mathew, S. Garcia, D. Karatzas, and C. V. Jawahar, “Reading between the lanes: Text videoqa on the road,” in *International Conference on Document Analysis and Recognition*, 7 2023, pp. 137–154. [Online]. Available: <http://arxiv.org/abs/2307.03948>
- [46] K. Chen, Y. Li, W. Zhang, Y. Liu, P. Li, R. Gao, L. Hong, M. Tian, X. Zhao, Z. Li, D.-Y. Yeung, H. Lu, and X. Jia, “Automated evaluation of large vision-language models on self-driving corner cases,” in *IEEE/CVF Winter Conference on Applications of Computer Vision*, 4 2025, pp. 7817–7826. [Online]. Available: <http://arxiv.org/abs/2404.10595>
- [47] X. Guo, R. Zhang, Y. Duan, Y. He, C. Zhang, S. Liu, and L. Chen, “Drivemllm: A benchmark for spatial understanding with multimodal large language models in autonomous driving,” 11 2024. [Online]. Available: <http://arxiv.org/abs/2411.13112>
- [48] X. Ding, J. Han, H. Xu, X. Liang, W. Zhang, and X. Li, “Holistic autonomous driving understanding by bird’s-eye-view injected multi-modal large models,” in *Proceedings of the IEEE/CVF Conference on Computer Vision and Pattern Recognition*, 2024, pp. 13 668–13 677. [Online]. Available: <https://github>.
- [49] K. Charoenpitaks, V.-Q. Nguyen, M. Suganuma, K. Arai, S. Totsuka, H. Ino, and T. Okatani, “Tb-bench: Training and testing multi-modal ai for understanding spatio-temporal traffic behaviors from dashcam images/videos,” 1 2025. [Online]. Available: <http://arxiv.org/abs/2501.05733>
- [50] T. Choudhary, V. Dewangan, S. Chandhok, S. Priyadarshan, A. Jain, A. K. Singh, S. Srivastava, K. M. Jatavallabhula, and K. M. Krishna, “Talk2bev: Language-enhanced bird’s-eye view maps for autonomous driving,” 10 2023. [Online]. Available: <http://arxiv.org/abs/2310.02251>
- [51] A. Gopalkrishnan, R. Greer, and M. Trivedi, “Multi-frame, lightweight and efficient vision-language models for question answering in autonomous driving,” 3 2024. [Online]. Available: <http://arxiv.org/abs/2403.19838>
- [52] J. Lübberstedt, E. Rivera, N. Uhlemann, and M. Lienkamp, “V3lma: Visual 3d-enhanced language model for autonomous driving,” 4 2025. [Online]. Available: <http://arxiv.org/abs/2505.00156>
- [53] X. Zhou, L. Shan, and X. Gui, “Dynrsl-vlm: Enhancing autonomous driving perception with dynamic resolution vision-language models,” 3 2025. [Online]. Available: <http://arxiv.org/abs/2503.11265>
- [54] A. Dosovitskiy, G. Ros, F. Codevilla, A. López, and V. Koltun, “Carla: An open urban driving simulator,” in *Conference on robot learning*, 2017, pp. 1–16.
- [55] H. Caesar, V. Bankiti, A. H. Lang, S. Vora, V. E. Liong, Q. Xu, A. Krishnan, Y. Pan, G. Baldan, and O. Beijbom, “nusscenes: A multimodal dataset for autonomous driving,” in *2020 IEEE/CVF Conference on Computer Vision and Pattern Recognition (CVPR)*. IEEE, 6 2020, pp. 11 618–11 628. [Online]. Available: <https://ieeexplore.ieee.org/document/9156412/>
- [56] H. Duan, J. Yang, Y. Qiao, X. Fang, L. Chen, Y. Liu, X. Dong, Y. Zang, P. Zhang, J. Wang *et al.*, “Vlmevalkit: An open-source toolkit for evaluating large multi-modality models,” in *Proceedings of the 32nd ACM International Conference on Multimedia*, 2024, pp. 11 198–11 201.
- [57] X. Lu, Y. Chen, C. Chen, H. Tan, B. Chen, Y. Xie, R. Hu, G. Tan, R. Wu, Y. Hu, Y. Zeng, L. Wu, L. Bian, Z. Wang, L. Liu, Y. Yang, H. Xiao, A. Zhou, Y. Wen, X. Chen, S. Ren, and H. Li, “Bluelm-v-3b: Algorithm and system co-design for multimodal large language models on mobile devices,” in *Proceedings of the Computer Vision and Pattern Recognition Conference*, 2025, pp. 4145–4155.
- [58] T. Wolf, L. Debut, V. Sanh, J. Chaumond, C. Delangue, A. Moi, P. Cistac, T. Rault, R. Louf, M. Funtowicz *et al.*, “Transformers: State-of-the-art natural language processing,” in *Proceedings of the 2020 conference on empirical methods in natural language processing: system demonstrations*, 2020, pp. 38–45.
- [59] S. Lu, Y. Li, Q.-G. Chen, Z. Xu, W. Luo, K. Zhang, and H.-J. Ye, “Ovis: Structural embedding alignment for multimodal large language model,” 5 2024. [Online]. Available: <http://arxiv.org/abs/2405.20797>
- [60] H. Dong, Z. Kang, W. Yin, X. Liang, C. Feng, and J. Ran, “Scalable vision language model training via high quality data curation,” 1 2025. [Online]. Available: <http://arxiv.org/abs/2501.05952>
- [61] Z. Chen, W. Wang, Y. Cao, Y. Liu, Z. Gao, E. Cui, J. Zhu, S. Ye, H. Tian, Z. Liu, L. Gu, X. Wang, Q. Li, Y. Ren, Z. Chen, J. Luo, J. Wang, T. Jiang, B. Wang, C. He, B. Shi, X. Zhang, H. Lv, Y. Wang, W. Shao, P. Chu, Z. Tu, T. He, Z. Wu, H. Deng, J. Ge, K. Chen, K. Zhang, L. Wang, M. Dou, L. Lu, X. Zhu, T. Lu, D. Lin, Y. Qiao, J. Dai, and W. Wang, “Expanding performance boundaries of open-source multimodal models with model, data, and test-time scaling,” 12 2024. [Online]. Available: <http://arxiv.org/abs/2412.05271>
- [62] W. Wang, Z. Chen, W. Wang, Y. Cao, Y. Liu, Z. Gao, J. Zhu, X. Zhu, L. Lu, Y. Qiao, and J. Dai, “Enhancing

- the reasoning ability of multimodal large language models via mixed preference optimization,” 11 2024. [Online]. Available: <http://arxiv.org/abs/2411.10442>
- [63] S. Gu, J. Zhang, S. Zhou, K. Yu, Z. Xing, L. Wang, Z. Cao, J. Jia, Z. Zhang, Y. Wang, Z. Hu, B.-W. Zhang, J. Li, D. Liang, Y. Zhao, S. Wang, Y. Ao, Y. Ju, H. Ma, X. Li, H. Diao, Y. Cui, X. Wang, Y. Liu, F. Feng, and G. Liu, “Infinity-mm: Scaling multimodal performance with large-scale and high-quality instruction data,” 10 2024. [Online]. Available: <http://arxiv.org/abs/2410.18558>
- [64] P. Wang, S. Bai, S. Tan, S. Wang, Z. Fan, J. Bai, K. Chen, X. Liu, J. Wang, W. Ge, Y. Fan, K. Dang, M. Du, X. Ren, R. Men, D. Liu, C. Zhou, J. Zhou, and J. Lin, “Qwen2-vl: Enhancing vision-language model’s perception of the world at any resolution,” 9 2024. [Online]. Available: <http://arxiv.org/abs/2409.12191>
- [65] A. Dosovitskiy, L. Beyer, A. Kolesnikov, D. Weissenborn, X. Zhai, T. Unterthiner, M. Dehghani, M. Minderer, G. Heigold, S. Gelly, J. Uszkoreit, and N. Houlsby, “An image is worth 16x16 words: Transformers for image recognition at scale,” 10 2020. [Online]. Available: <http://arxiv.org/abs/2010.11929>
- [66] J. Su, Y. Lu, S. Pan, A. Murtadha, B. Wen, and Y. Liu, “Roformer: Enhanced transformer with rotary position embedding,” *Neurocomputing*, vol. 568, 4 2024. [Online]. Available: <http://arxiv.org/abs/2104.09864>
- [67] N. Shazeer, A. Mirhoseini, K. Maziarz, A. Davis, Q. Le, G. Hinton, and J. Dean, “Outrageously large neural networks: The sparsely-gated mixture-of-experts layer,” 1 2017. [Online]. Available: <http://arxiv.org/abs/1701.06538>
- [68] J. Wei, X. Wang, D. Schuurmans, M. Bosma, B. Ichter, F. Xia, E. Chi, Q. Le, and D. Zhou, “Chain-of-thought prompting elicits reasoning in large language models,” *Advances in neural information processing systems*, vol. 35, pp. 24 824–24 837, 1 2022. [Online]. Available: <http://arxiv.org/abs/2201.11903>
- [69] E. W. Noreen, *Computer-intensive methods for testing hypotheses*. Wiley New York, 1989.
- [70] A. Yang, B. Yang, B. Zhang, B. Hui, B. Zheng, B. Yu, C. Li, D. Liu, F. Huang, H. Wei, H. Lin, J. Yang, J. Tu, J. Zhang, J. Yang, J. Yang, J. Zhou, J. Lin, K. Dang, K. Lu, K. Bao, K. Yang, L. Yu, M. Li, M. Xue, P. Zhang, Q. Zhu, R. Men, R. Lin, T. Li, T. Tang, T. Xia, X. Ren, X. Ren, Y. Fan, Y. Su, Y. Zhang, Y. Wan, Y. Liu, Z. Cui, Z. Zhang, and Z. Qiu, “Qwen2.5 technical report,” 2024.
- [71] T. Dao, “Flashattention-2: Faster attention with better parallelism and work partitioning,” in *The Twelfth International Conference on Learning Representations*, 2024.



vision-language models

NIKOS THEODORIDIS (Graduate Student Member, IEEE) received the B.Sc. degree in physics from the Aristotle University of Thessaloniki, Thessaloniki, Greece, in 2023, and the M.Sc. degree in artificial intelligence and machine learning from the University of Limerick, Limerick, Ireland, in 2024. He is currently working toward the full-time Ph.D. degree with the Department of Electronic and Computer Engineering, University of Limerick, Limerick, Ireland. His research interests include



TIM BROPHY (Member, IEEE) received the B.Eng. (Hons.) degree from the University of Galway in 2018. From 2018 to 2025, he was a member of the Connaught Automotive Research (CAR) Group at the University of Galway, where he completed his PhD studies. In 2025, he joined the University of Limerick as a Postdoctoral Researcher. His research interests include sensor availability, computer vision, and artificial intelligence in the context of automated vehicles.



and edge deployment of deep learning algorithms.

REENU MOHANDAS (Member, IEEE) received the M.Tech. degree in digital image computing from the University of Kerala, India, in 2014, the M.Sc. degree in artificial intelligence from CIT, currently Munster Technological University, Cork, Ireland, in 2019, and Ph.D. from the Department of Electronic and Computer Engineering (ECE), University of Limerick, Ireland, and currently a Postdoctoral Researcher there. Her research interests include computer vision, deep learning, incremental learning, VQA models, and quantisation



Foundation Ireland’s Data Science Ph.D. degree and the National M.Sc. degree in AI programs with the University of Limerick, blending academic insight with industry expertise.

GANESH SISTU is currently a Principal AI Architect with Valeo, Tuam, Ireland, and also an Adjunct Assistant Professor with the University of Limerick, Limerick, Ireland. He is leading Multiple Global Research Teams working on automated driving and parking. With more than 14 years in computer vision and machine learning, he has authored or coauthored more than 35 publications in top-tier conferences like ICCV and ICRA. He plays a pivotal role in guiding the future of AI education as an Industry Board Member for Science



postdoctoral research from 2011-2014. His research interests are in computer vision and data analytics.

Fiachra Collins received his B.E. degree in Mechanical Engineering from University College Dublin in 2007 and PhD degree from Dublin City University in 2011. Since 2019, he has been the Geometric Perception Team Manager in Valeo Vision Systems, overseeing the software development for camera calibration and perception algorithms (3D reconstruction, localization, mapping). Prior to Valeo, from 2014-2018 he was Chief Technology Officer for a start-up company specializing in IoT and sensors, which was a spin-out of his



ANTHONY SCANLAN received the B.Sc. degree in experimental physics from the National University of Ireland Galway, Galway, Ireland, in 1998, and the M.Eng. and Ph.D. degrees in electronic engineering from the University of Limerick, Limerick, Ireland, in 2001 and 2005, respectively. He is currently a Senior Research Fellow with the Department of Electronic and Computer Engineering, University of Limerick, and has been the Principal Investigator on several research projects in the areas of signal processing and data converter

design. His current research interests include artificial intelligence, computer vision, and industrial and environmental applications.



CIARAN EISING (Senior Member, IEEE) received the B.E. degree in electronic and computer engineering and the Ph.D. degree from the NUI Galway, Galway, Ireland, in 2003 and 2010, respectively. From 2009 to 2020, he was a Computer Vision Architect and Senior Expert with Valeo. In 2020, he joined the University of Limerick, Limerick, Ireland, as an Associate Professor.